On point-sets that support planar graphs ☆

V. Dujmović [a], W. Evans [b], S. Lazard [c], W. Lenhart [d], G. Liotta [e], D. Rappaport [f], S. Wismath [g],*

[a] *Carleton University, Canada*
[b] *University of British Columbia, Canada*
[c] *INRIA Nancy, LORIA, France*
[d] *Williams University, USA*
[e] *Universitá degli Studi di Perugia, Italy*
[f] *Queen's University, Canada*
[g] *University of Lethbridge, Canada*

ARTICLE INFO

ABSTRACT

A universal point-set supports a crossing-free drawing of any planar graph. For a planar graph with n vertices, if bends on edges of the drawing are permitted, universal point-sets of size n are known, but only if the bend points are in arbitrary positions. If the locations of the bend points must also be specified as part of the point-set, we prove that any planar graph with n vertices can be drawn on a universal set $\mathcal{S}$ of $O(n^2/\log n)$ points with at most one bend per edge and with the vertices and the bend points in $\mathcal{S}$. If two bends per edge are allowed, we show that $O(n \log n)$ points are sufficient, and if three bends per edge are allowed, $O(n)$ points are sufficient. When no bends on edges are permitted, no universal point-set of size $o(n^2)$ is known for the class of planar graphs. We show that a set of n points in balanced biconvex position supports the class of maximum-degree-3 series-parallel lattices.

1. Introduction

A set of points *supports* the drawing of a graph G if there is a one-to-one mapping f of the vertices of G to the points so that for all pairs of edges $(a, b), (c, d)$ in G (where a, b, c, d are distinct), segments $\overline{f(a)f(b)}$ and $\overline{f(c)f(d)}$ do not intersect. A set of points that supports the drawing of all n-vertex graphs in some class is called *cuniversal* for that class, or simply *universal* if the class is all planar graphs. The size of any universal point-set for planar graphs requires at least $1.235n$ points as shown by Kurowski [1] (see also Chrobak and Karloff [2]). Early graph drawing results, such as the canonical ordering technique of de Fraysseix, Pach, Pollack [3] and Schnyder's embedding [4] demonstrate that an $n \times n$ grid of points is a universal point-set. However, no universal point-set of size $o(n^2)$ is known.

Smaller universal point-sets for sub-classes of planar graphs are known. For example, any outerplanar graph can be drawn on *any* set of n points in general position [5]. Indeed, if the point-set is in convex position, then it supports exactly the family of outerplanar graphs. Determining other families of planar graphs for which universal point-sets of size n exist is an interesting problem. We examine a particular type of point-set, of size n, in which points are arranged in biconvex position, and show that it supports the drawing of all maximum-degree-3 series-parallel lattices, a class of graphs that contains members that are not outerplanar.

Table 1

Summary of results – cardinality of universal point-sets for classes of graphs. The first and last results are well known. All other results are new.

Graphs	Number of points	Number of bends	Reference
Outerplanar	n	0	[5]
3SP lattice	n	0	Theorem 1
Planar	$O(n)$	3	Theorem 2
Planar	$O(n \log n)$	2	Theorem 2
Planar	$O(n^2 / \log n)$	1	Theorem 2
Sub-Hamiltonian	$O(n \log n)$	1	Section 2.2
Sub-Hamiltonian	$O(n)$	2	Section 2.1
Planar	$O(n^2)$	0	[3,4]

The main contributions in this paper are stated in Theorems 1 and 2, and pertain to universal point-sets for straight-line drawings, and drawings with bends respectively.

Theorem 1. *For all n, there exist universal point-sets of cardinality n that support the family of maximum-degree-3 series-parallel lattices with n vertices.*

Suppose we relax the definition of *support* to allow edges of the graph to map to polylines composed of (at most) $k+1$ line segments. In other words, we allow edges that "bend" at most k times. In this case, universal point-sets of size n exist for two bends [6] and even one bend [7]. However, these results assume that the bend points can be placed in arbitrary locations and these bend points are not included as part of the universal point-set. It is natural to ask if there exists a point-set that supports all planar graphs where each vertex *and each bend point* occurs at a point in the set. As before, we require all pairs of edges (a, b) and (c, d) (where a, b, c, d are distinct) to map to non-intersecting polylines. Previous to this paper, no such point-set of cardinality $o(n^2)$ was known for any value of k. Extending the results of [7] and [6] in a straightforward manner imply point-sets of size $O(n^3)$. For $k = 3, 2, 1$, we present such universal point-sets of cardinality $O(n)$, $O(n \log n)$, and $O(n^2 / \log n)$ respectively. Our analyses of these cardinalities are tight; no lower bounds other than $\Omega(n)$ are known for these cases.

Theorem 2. *For all n, there exist universal point-sets of cardinality $O(n)$, $O(n \log n)$, and $O(n^2 / \log n)$ that support the drawing of all n-vertex planar graphs with at most three, two, or one bend per edge, respectively.*

The paper is organized as follows. In Sections 2.1, 2.2, 2.3 the effect of allowing bend points on edges is considered, when the bend points must also be located at points of the supporting point-set. Universal point-sets are constructed for three cases: when at most three, two, or one bend(s) per edge are permitted, thus establishing Theorem 2. One consequence of our construction is that the class of sub-Hamiltonian graphs (i.e. a planar graph that can be made Hamiltonian by the addition of edges while preserving planarity) can be universally supported efficiently (i.e. with fewer bends).

In Section 3 a particular point-set (called biconvex) of size n is considered and we show a class of planar graphs for which it is universal. An application of this result to simultaneous embeddings and other consequences are discussed. Table 1 summarizes our results in terms of which sets of planar graphs can be supported on point-sets of a given cardinality with a specified number of bends.

We adopt standard notation from the graph drawing literature and we assume all graphs have n vertices.

Two of our results rely on point-sets that have a specific form; see, for example, Fig. 10. Two non-intersecting non-linear curves λ_1 and λ_2 are defined to be *biconvex* if: each of the curves λ_1 and λ_2 is convex, the convex hull of the 4 endpoints of the two curves completely contains the two curves, and the line segment joining any point a of λ_1 to any point b of λ_2 does not intersect either curve except at a and b.

Without loss of generality, we assume the existence of a horizontal line separating the two curves with λ_1 below λ_2. A point-set all of whose points lie on two curves that are biconvex is said to be in *biconvex position*. We note that point-sets in such a configuration have been used in other contexts under different names, for example as a *double-chain* in the triangulation enumeration literature.

2. Universal point-sets for drawing planar graphs with bends

In this section we establish Theorem 2 by constructing universal point-sets for each of the three cases: 3, 2 or 1 bend per edge allowed. A fundamental tool in our constructions for universal point-sets with bends is the following result proving the existence of a book embedding of planar graphs in which the edges are permitted to cross the spine [8]. A *monotone topological book embedding* of a planar graph G is a planar drawing such that all vertices of G are represented as distinct points on a *spine* (i.e. the x-axis), and each edge is either represented as an arc in the bottom page (below the x-axis), or as an arc in the top page (above the x-axis), or as the concatenation of two arcs: the first (leftmost) in the bottom page and the second in the top page with their common crossing point between spine points. See Fig. 1.
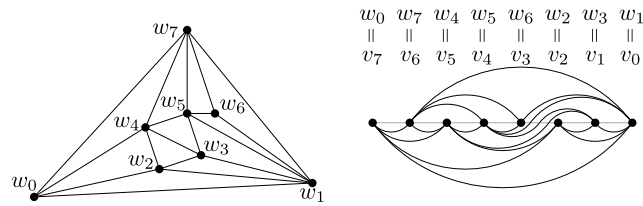
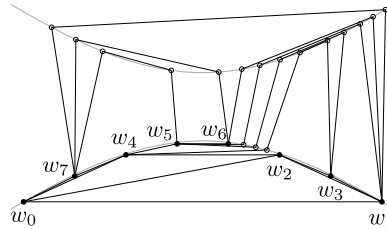**Fig. 1.** A graph and a monotone topological book embedding of it.

Fig. 2. Example of an embedding of the graph of Fig. 1 on a biconvex point-set using three bends per edge. The circles on the upper curve are the bend points $b_1, \ldots, b_{2a}$. The circles on the lower curve are bend points at dummy vertices. For clarity, the curvature is exaggerated and only the first 14 of the 36 upper curve points and 11 of the 26 lower curve points in the universal point-set are shown.

Theorem 3. *(See [8].) Every planar graph has a proper monotone topological book embedding which can be computed in time linear in the size of the graph.*

2.1. A set of $\Theta(n)$ points for drawing planar graphs with 3 bends per edge

Lemma 4. *There exists a universal set of $10n - 18$ points that supports the drawing of planar graphs with 3 bends per edge.*

Proof. Before introducing the (fixed) universal point-set, we first outline how the graph will be processed. Consider a proper monotone topological book embedding of the input graph. For each edge that intersects the spine, introduce a dummy vertex creating an *augmented two page book embedding* with the vertices of the spine drawn on a horizontal line. There are at most $n + m \leqslant 4n - 6$ vertices on the spine. Imagine a horizontal line slightly above the spine that intersects all arcs in the top page – call these points of intersection from left to right $b_1, \ldots, b_{2a}$ where a is the number of arcs. Note that $a \leqslant 3n - 6$.

Consider a point-set that lies on two curves in biconvex position and consists of $6n - 12$ points on the top curve and $4n - 6$ points on the bottom curve. We prove that any such point-set is universal for drawing planar graphs with at most three bends per edge. For any specific graph, its augmented two page book embedding defines the drawing and requires at most $10n - 18$ points. The at most $4n - 6$ vertices on the spine (including dummy vertices) are assigned, in order, to the first points on the bottom curve. The bend points $b_1, \ldots, b_{2a}$ are assigned to the first $2a$ points of the upper curve in left to right order and then each arc in the top page is drawn using the associated bend points. These polylines do not intersect since the upper curve is convex and any segment joining the two curves does not properly intersect these curves. The arcs in the bottom page can be drawn with no bends – they are chords of the bottom curve. Each arc in the top page uses two bend points. Substituting a bend point for each of the dummy vertices results in a drawing with at most three bends per edge. Refer to Fig. 2 for an example of the construction. □

Note that a sub-Hamiltonian planar graph corresponds exactly to a graph that has a two page (unaugmented) book embedding [8]. Since such graphs do not require dummy vertices, they can be drawn with at most two bends per edge.

2.2. A set of $\Theta(n \log n)$ points for drawing planar graphs with 2 bends per edge

Before describing our universal point-sets for the two bend case, we describe the geometric idea underlying our construction. Similar to Section 2.1, we draw the spine vertices of an augmented two page book embedding on a set of points that lie on a slightly concave curve close to the x-axis. This implies that all the arcs in the bottom page of the book embedding can be drawn as straight line segments. For arcs in the top page, if the arc is from the ith to the $(i + j)$th spine vertex, it is drawn to bend at a point at level j. We place approximately n/j bend points approximately equally spaced in the x-dimension at level j, since only n/j top arcs can have "length" j. The bend point that lies between the ith and $(i + j)$th spine vertices is used by this arc. Each level is at a y-coordinate that is large enough that the drawing of an arc that uses a bend point at a lower level "nests" inside any drawing of an arc from the same vertex using a higher level bend point. Of course, for each $j > n/2$, there can be only one arc of "length" j and it uses a single bend point at level j. The total number of bend points we place is $O(n \log n)$.
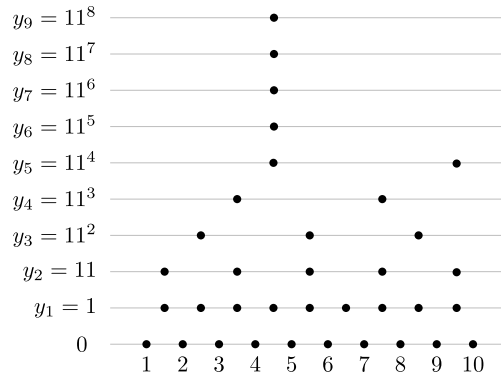
Fig. 3. A 2-bend universal point-set for 4-vertex planar graphs. The y-axis is not to scale.

Lemma 5. *There exists a universal set of $\Theta(n \log n)$ points that supports the drawing of planar graphs with 2 bends per edge.*

Proof. Let $N = 4n - 6$ and refer to Fig. 3. The following point-set is a 2-bend-universal point-set for n-vertex planar graphs: Place points at $(x, 0)$ for $x = 1, \ldots, N$. (Actually, place points at $(x, \frac{x(N-x)}{N^2})$ so that they lie on a slightly concave curve, but for clarity we omit this technical detail in the following.) Let $g(i, j) = j \lfloor \frac{i}{j} \rfloor$. For $j = 1, 2, \ldots, N$, place the set of points $\{(g(i, j) + \min\{j, \frac{N}{2}\} - \frac{1}{2}, y_j) \mid i = 1, 2, \ldots, N - j\}$ (avoiding duplicates) where y_j satisfies $y_1 = 1$ and $y_{j+1} > N y_j$ for $1 \leqslant j < N - 1$. Notice that the number of points on line y_j is at most $\lfloor \frac{N}{j} \rfloor$ since it is the number of distinct values of $\lfloor \frac{i}{j} \rfloor$ for $1 \leqslant i \leqslant N - j$, which is at most $1 + \lfloor \frac{N-j}{j} \rfloor = \lfloor \frac{N}{j} \rfloor$. Fig. 3 shows the set of points for $n = 4$.

To embed a given n-vertex planar graph G, first construct a proper monotone topological book embedding of G with vertices on the x-axis and introduce dummy vertices on the arcs that cross the x-axis. Let G' be the resulting graph, which has (at most) $3n - 6$ additional vertices and arcs. Place the vertices of G' on the points $(x, 0)$, $x = 1, \ldots, N$, preserving their order from the book embedding. Let v_x be the vertex at point $(x, 0)$.

For every arc (v_i, v_{i+j}) in G' above the x-axis in the book embedding, draw a one-bend polyline from $(i, 0)$ to $(g(i, j) + \min\{j, \frac{N}{2}\} - \frac{1}{2}, y_j)$ to $(i + j, 0)$. For every arc (v_i, v_{i+j}) in G' below the x-axis in the book embedding, draw the straight polyline from $(i, 0)$ to $(i + j, 0)$. We will show that no two polylines above the x-axis cross in this drawing by an analysis of the slopes of the segments of the polylines.

For *any* arc (v_i, v_{i+j}) above the x-axis in G', let Δ_x and Δ_y be the difference in the x- and y-coordinates respectively of v_i and the bend point of arc (v_i, v_{i+j}). We first show that $\frac{1}{2} \leqslant \Delta_x \leqslant \frac{N}{2}$. If $j \leqslant \frac{N}{2}$, then $\Delta_x = g(i, j) + j - \frac{1}{2} - i$ and, by definition, $0 \leqslant i - g(i, j) \leqslant j - 1$, thus $\Delta_x \in [1 - j + j - \frac{1}{2}, j - \frac{1}{2}] \subseteq [\frac{1}{2}, \frac{N}{2}]$. If $j > \frac{N}{2}$, then $i < \frac{N}{2}$ (otherwise $i + j > N$), thus $i < j$ and $g(i, j) = 0$; thus $\Delta_x = 0 + \frac{N}{2} - \frac{1}{2} - i$ which is less than $\frac{N}{2}$ and at least $\frac{1}{2}$ since $i < \frac{N}{2}$ and thus $i \leqslant \frac{N}{2} - 1$ (since N is even).

Consider now two arcs (v_i, v_{i+j}) and $(v_{i'}, v_{i'+j'})$ above the x-axis where $i \leqslant i'$. Since the arcs do not intersect in the book embedding, we have $i' + j' \leqslant i + j$, and so $0 \leqslant i' - i \leqslant j - j'$ with at least one inequality being strict (otherwise the two arcs have identical endpoints). Thus $j' < j$. We now show that the slope of the initial segment of the polyline for arc (v_i, v_{i+j}) is greater than that of the first segment for arc $(v_{i'}, v_{i'+j'})$ and that the slope of the second segment of the polyline for arc (v_i, v_{i+j}) is less than that of the one for arc $(v_{i'}, v_{i'+j'})$. Since the first segments of each polyline have positive slopes and the second segments have negative slopes, the polylines do not intersect above the x-axis, that is, the "nesting" of the book embedding arcs is preserved.

Again, defining Δ_x and Δ_y as above for the first segment of the polyline in G' of arc (v_i, v_j), and defining similarly Δ'_x and Δ'_y for the first segment of the polyline in G' of arc $(v_{i'}, v_{i'+j'})$, we have that both $\frac{1}{2} \leqslant \Delta_x \leqslant \frac{N}{2}$ and $\frac{1}{2} \leqslant \Delta'_x \leqslant \frac{N}{2}$. This implies that $\Delta_x \leqslant \frac{N}{2} \leqslant N \Delta'_x$. On the other hand, $y_j \geqslant y_{j'+1} > N y_{j'}$, thus $\Delta_y > N \Delta'_y$. Hence, $\frac{\Delta_y}{\Delta_x} > \frac{N \Delta'_y}{N \Delta'_x}$, which is our slope requirement for the segments incident to v_i and $v_{i'}$ in arcs (v_i, v_{i+j}) and $(v_{i'}, v_{i'+j'})$ respectively. A similar argument establishes our slope requirement for the segments incident to v_{i+j} and $v_{i'+j'}$ in arcs (v_i, v_i) and $(v_{i'}, v_{i'+j'})$ respectively. Note also that $\frac{\Delta_y}{\Delta_x} > \frac{1}{N}$ (since $\Delta_y \geqslant 1$ and $\Delta_x \leqslant \frac{N}{2}$), thus the segments do not properly intersect the slightly concave arc of parabola which support the vertices v_i and whose slope is in $[-\frac{1}{N}, \frac{1}{N}]$ for x in $[0, N]$.

Such a universal point-set consists of at most $N + \sum_{j=1}^{N} \lfloor \frac{N}{j} \rfloor = \Theta(N \log N) = \Theta(n \log n)$ points as candidate bend points for edges in the top page, and $4n - 6$ points on the x-axis to support the augmented spine. □

Sub-Hamiltonian graphs require only one bend per edge using this construction, since they have a book embedding containing no dummy vertices.
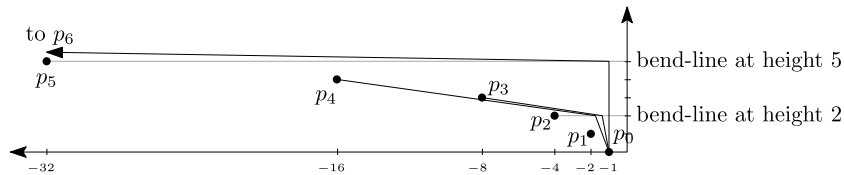
Fig. 4. The one-bend drawing of the three edges, in the top page or crossing the spine, and incident to $v_0 = w_1$ in the graph of Fig. 1 following the construction of [7]. The points p_6 and p_7 are not shown since the figure is to scale.

2.3. A set of $\Theta(n^2/\log n)$ points for drawing planar graphs with 1 bend per edge

In [7], the authors describe a universal set of n points on which all planar graphs with n vertices can be drawn with at most one bend per edge. Although not noted in that paper, their construction trivially yields a universal set of size $\Theta(n^3)$ of points for the bend locations. We show here how to reduce the size of the universal set of bend points to $\Theta(n^2/\log n)$ while preserving a linear size universal set of points for the vertices. Our construction being similar to that in [7], we recall briefly this construction, referring to Figs. 1 and 4.

Given a planar graph G with n vertices, we embed the graph on vertices $p_i = (-2^i, i)$ for $i = 0, \ldots, n-1$ with at most one bend per edge, as follows. We first compute a proper monotone topological book embedding, Γ of G. We relabel the vertices of that book embedding from right to left, as $v_0, \ldots, v_{n-1}$. We then map these vertices to $p_0, \ldots, p_{n-1}$, respectively. All the edges below the spine are drawn as straight-line segments. The others are drawn with a bend point as follows: Consider an edge whose rightmost vertex is v_i and that intersects the spine on the interval $[v_{u+1}, v_u)$ (inclusive of v_{u+1} – which is left of v_u – for the case where the leftmost endpoint of the edge is v_{u+1}). Such an edge is drawn with a bend point on the horizontal line through p_u and in the vertical strip delimited by p_i and p_{i+1} (recall that the v_i are drawn at the p_i). In what follows, the horizontal line through p_u is called the *bend line* through p_u. This construction requires a set of candidate bend points of size $\Theta(n^3)$ since inside every vertical strip, on every bend line, there need to be up to $n - i - 1$ candidate bend points (for every possible edge with right endpoint p_i).

We show how this construction can be modified to contain only a subquadratic universal set of points for the bends while preserving a linear size universal set of points for the vertices.

Lemma 6. *There exists a universal set of $\Theta(n^2/\log n)$ points that supports the drawing of planar graphs with 1 bend per edge.*

Proof. The proof is organized as follows. We first add some isolated "dummy" vertices in the topological book embedding Γ of the input graph G. With a slight modification of the construction of [7], we can reduce the number of candidate bend points in each vertical strip bounded by p_{i+1} and p_i to at most one per bend line, resulting in an overall total of $\Theta(n^2)$; moreover, no drawing will use more than one candidate bend point from any bend line.

We then show how we can reduce the number of candidate bend points from $\Theta(n^2)$ to $\Theta(n^2/\log n)$. We do this by first describing our construction of a universal set of points for the bends, then proving that the size of this set is $\Theta(n^2/\log n)$, then verifying that the construction of [7] (slightly modified to only use the reduced number of candidate bend points) is still valid. This final step of verifying that the (slightly modified) construction of [7] gives a crossing-free drawing of any planar graph on our universal point-set is almost the same as in [7]. Since this proof is fairly long – though not particularly difficult – we do not duplicate it here; instead we give an alternate argument by describing motions of the bend points in the construction of [7] to locations in our $\Theta(n^2/\log n)$ point-set that do not introduce any crossings. □

2.3.1. Augmented topological book embedding

We consider, as in [7], a proper monotone topological book embedding Γ of our input graph G (see Fig. 1). On the spine of Γ, add isolated *dummy vertices* as follows (see Fig. 5(a)): Between any two vertices v and w of G that are consecutive on the spine of Γ, with v to the left of w, add d_v dummy vertices to the spine of Γ, where d_v is the number of edges of G that cross the spine between v and w plus the number of top-page edges of Γ having leftmost endpoint v. More precisely, in the interval (v, w), we add on the spine one dummy vertex between each pair of consecutive spine-crossing edges as well as between the rightmost spine-crossing edge and w; the remaining vertices are added between v and the leftmost spine-crossing edge (or between v and w if there is no spine-crossing edge). If w is mapped to p_i, then the dummy vertices will be mapped to $p_{i+1}, \ldots, p_{i+d_v}$ and v will be mapped to p_{i+d_v+1}, providing a separate bend line for each edge intersecting the segment $[p_{i+d_v+1}, p_i)$ and guaranteeing that at most one bend point is drawn on every bend line (though the bend line supports many *candidate* bend points). Since the number of edges of a planar graph is at most $3n - 6$, we add at most that number of isolated vertices and the total number of vertices is less than $4n$. Let Γ' be the resulting graph.

2.3.2. Modification of the construction of [7] leading to $\Theta(n^2)$ candidate bend points

We show how a slight modification of the construction of [7] on this augmented graph Γ' leads to a quadratic universal set of points for the bends. Refer to Fig. 5(b). Since Γ' has no more than $4n$ vertices, we construct a set of $4n$ points $p_0, \ldots, p_{4n-1}$ as in [7] that will support the vertices $v_0, v_1, \ldots$ of any augmented graph Γ'. We assume from this point
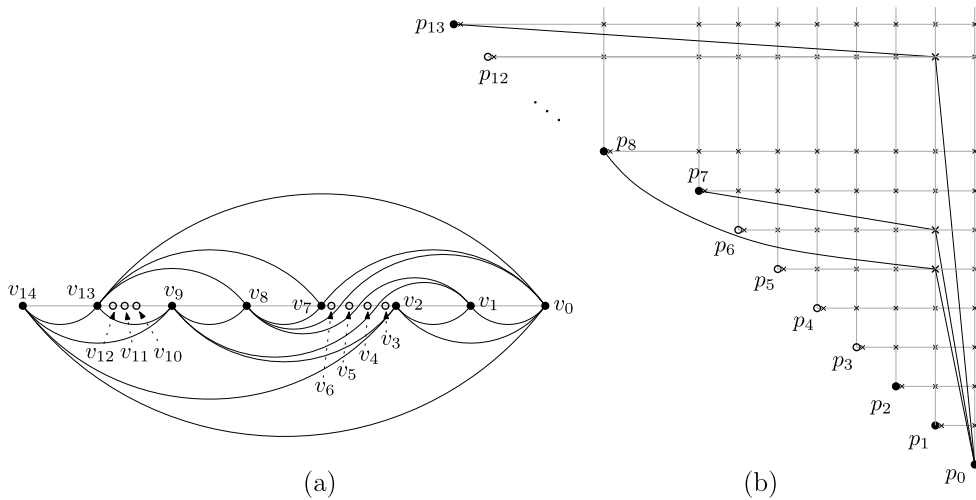
Fig. 5. (a) Augmented topological book embedding Γ' of the graph Γ of Fig. 1. The isolated dummy vertices are drawn as circles. (b) One-bend drawing of the three top-page or spine-crossing edges incident to v_0 of Γ' (the same edges as in Fig. 4) in the construction using $\Theta(n^2)$ candidate bend points, which are drawn as crosses; one arc is drawn curved because the figure is not to scale.

on that each vertex v_i of Γ' is mapped to the point p_i. We then place vertically above every point p_i one candidate bend point on every bend line. More precisely, we place candidate bend points at integer heights between $i + 1$ and $n - 1$ above p_i, and, since we do not want to consider a candidate bend point that coincides with p_i, we place one to the right of p_i (at the same height) and sufficiently close to p_i. These points will serve as candidate bend points in the vertical strip delimited by p_i and p_{i-1}, that is, every top-page edge or spine-crossing edge of Γ' having rightmost endpoint v_{i-1} will use one of these bend points. All the edges of Γ' that are below the spine are drawn as straight-line segments, as explained above and as in [7]. We now describe how to draw the edges that lie at least partially above the spine.

Let v_i represent an original (non-dummy) vertex of G and let $v_{i-1}, \ldots, v_{i-d_{v_i}}$ represent the dummy vertices to the right of v_i (thus $v_{i-d_{v_i}-1}$ is the next original vertex of G to the right of v_i on the spine of Γ'). Now consider the collection of d_{v_i} edges of G that gave rise to these dummy vertices; they are the top-page edges having left endpoint v_i along with the edges that cross the spine of Γ between vertices v_i and $v_{i-d_{v_i}-1}$. Denote these edges by $e_1, \ldots, e_{d_{v_i}}$, where the first edges to appear in the list are the edges with left endpoint v_i, ordered by their clockwise order at v_i, and the last edges to appear in the list are those that cross the spine between v_i and $v_{i-d_{v_i}-1}$ in the (left to right) order that they cross the spine. Each edge e_k in this list will have its bend point on the bend line at height $i - k$ (that is, the bend line through p_{i-k}); if the right endpoint of edge e_k is v_r, then e_k will use the candidate bend point vertically above p_{r+1}. For each edge e in G, denote by $h(e)$ the height of the bend point for edge e in the drawing. Note that at most one bend point from any bend line will be used, and thus that $h(\cdot)$ induces a total ordering on the top-page and spine-crossing edges of Γ'. Moreover, this ordering (for decreasing $h(\cdot)$) is the same as the ordering obtained by concatenating, for all vertices of Γ' considered from left to right, the edges $e_1, \ldots, e_{d_{v_i}}$ in the order described above.

To understand why no two of the one-bend polylines intersect properly, we describe a motion that carries the bend points in the original construction of [7] to the bend points in our construction. We consider two consecutive motions. The first one ensures that bend points end up being drawn on distinct bend lines. Note that in the original construction the bend points of two edges of Γ' are drawn on the same bend line if and only if both edges have the same leftmost endpoint or if they intersect the spine between the same two consecutive vertices; by definition of the dummy vertices of Γ', this may only happen for two top-page edges that share the same left endpoint.

Consider then a vertex v_i that is the left endpoint of k edges in the top page of Γ'. Denote these edges by $e_1, \ldots, e_k$ in their *counterclockwise* order at v_i. These edges (in order) are drawn in the original construction with bend points, ordered from left to right, at the height of p_{i-1}. Considering the edges $e_1, \ldots, e_k$ in that order, we move the bend point of e_j along its rightmost segment in the direction of its rightmost endpoint until it reaches height $h(e_j)$ (i.e., we shorten the rightmost segment). All movements take place in the quadrilateral region bounded from above and on the right by edge e_k (whose bend point does not move), from below by the horizontal line through p_i, and on the left by the segment $p_i p_{i-k}$. Since no edges other than $e_1, \ldots, e_k$ intersect that region, we do not create any intersections during the motion. Furthermore, at the end of this motion, no two bend points lie on the same bend line.[1] For the second motion, consider any point p_i. All the edges whose right endpoint is p_i have their bend point drawn in the vertical strip bounded by the vertical lines through

---

[1] During this motion, edges $e_1, \ldots, e_k$ may sweep over some vertices in $p_{i-1}, \ldots, p_{i-k+1}$. We thus do not ensure that the topology (actually, the isotopy) of the augmented graph Γ' is preserved, but this is not an issue since the dummy vertices $v_{i-1}, \ldots, v_{i-k+1}$ are not part of the input graph G and thus are not ultimately drawn.
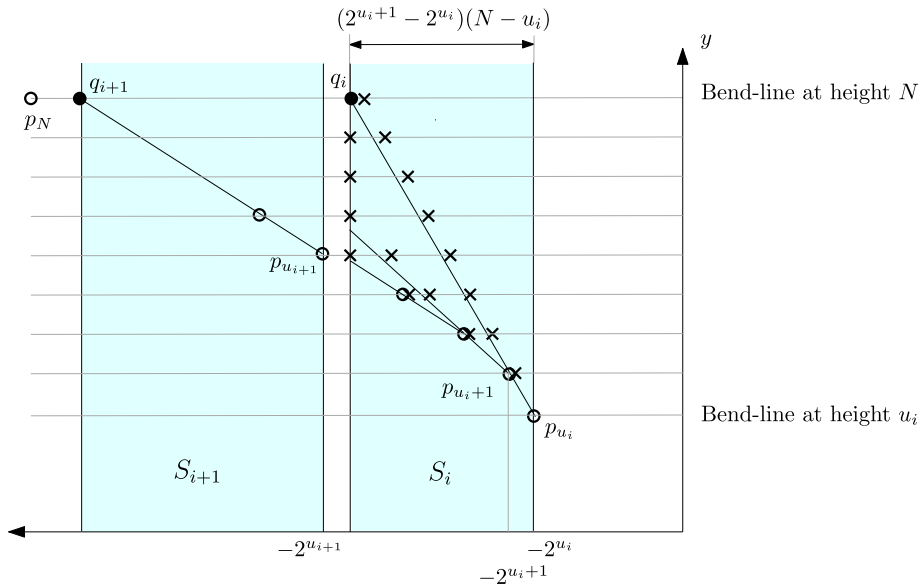
Fig. 6. Placement of candidate bend points in the strip S_i. The figure is not to scale.

p_{i+1} and p_i. We can thus move these bend points to the left boundary of the strip, without creating any intersection by moving them one by one, starting in every strip by the bottommost bend points.[2] This motion results in the drawing we described above.

2.3.3. Construction of a $\Theta(n^2/\log n)$ size universal set for the bend points

We obtain a subquadratic-size universal set of points as follows. As above, we construct a set P of $4n$ points $p_0, \ldots, p_{4n-1}$ as in [7] that will support the vertices of any augmented graph Γ'. We then define a set of vertical strips $S_0, \ldots, S_m$, where $m \in \Theta(n/\log n)$, that are disjoint and that together contain all of the points $p_0, \ldots, p_{4n-2}$ (and possibly contain p_{4n-1} as well). For each vertical strip S_i we will describe how to place $\Theta(n)$ candidate bend points in S_i which will be used by edges with right endpoint in S_i while avoiding intersections among edges. Note that S_m may also contain p_{4n-1} but it need not since p_{4n-1} is not the right endpoint of any edge. The drawing of Γ' will then be obtained, from the drawing using $\Theta(n^2)$ candidate bend points, by moving every bend point to the left (on the same bend line) until it reaches one (not necessarily the first one) of the new $\Theta(n^2/\log n)$ candidate bend points.

Let $N = 4n - 1$, the height of p_{4n-1}, and refer to Fig. 6. We simultaneously construct a subsequence $p_{u_0}, \ldots, p_{u_m}$ of P along with a set $q_0, \ldots, q_m$ of points on the bend line at height N such that q_i and p_{u_i} define the left and right boundaries, respectively, of S_i.

Let $u_0 = 0$, so $p_{u_0} = p_0$. The point q_0 is defined to be the intersection of the bend line at height N with the line $p_{u_0}p_{u_0+1} = p_0p_1$. Let p_{u_1} be the rightmost point of $p_0, \ldots, p_{4n-1}$ that is to the left of q_0 (or vertically aligned with q_0). The second point q_1, is the intersection of the bend line at height N with the line $p_{u_1}p_{u_1+1}$. Inductively, the point p_{u_i} is used to define q_i, as the point at which the bend line at height N intersects the line through p_{u_i} and p_{u_i+1}; q_i is then used to define $p_{u_{i+1}}$ as the rightmost p_j to the left of q_i (or vertically aligned with q_i). The construction ends at the first value of m for which q_m is to the left of p_{4n-2}.

Before proving that the number of vertical strips $S_0, \ldots, S_m$ is in $\Theta(n/\log n)$, we complete the description of our set of candidate bend points. Refer to Fig. 6. Consider the vertical strip S_i bounded by q_i on its left side and p_{u_i} on its right side (we assume S_i is open on its left side and closed on its right side). For each pair p_j, p_{j+1} of consecutive points of P in S_i, define $L_{i,j}$ to be the portion of the line p_jp_{j+1} that has p_j as its right endpoint and the intersection of line p_jp_{j+1} with the vertical line through q_i as its left endpoint. Near each point on segment $L_{i,j}$ having integer height strictly larger than j, we place a candidate bend point at that height and infinitesimally to the right of $L_{i,j}$. We do this so that the segments from candidate bend points to p_j do not overlap, and so that the candidate bend point at height $j + 1$ is distinct from p_{j+1}. Moreover, we require that between two of these candidate bend points, the higher ones are moved to the right more than the lower ones, so that a segment connecting p_j to a lower bend point is below any segment connecting p_j to a higher

---

[2] To avoid placing a bend point exactly at the location of p_{i+1}, we specify that the bend point at height p_{i+1} be moved to the left until it is slightly to the right of p_{i+1}.
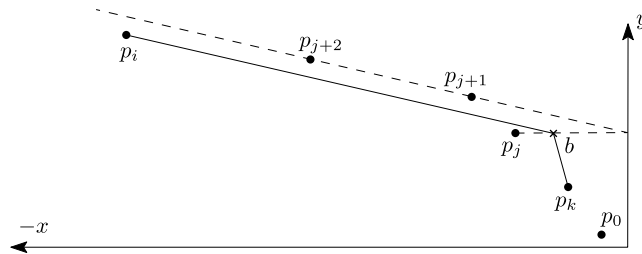
Fig. 7. The segment $p_i b$ intersects the segment $p_j p_{j+1}$. The figure is not to scale.

bend point. We also place a candidate bend point at every point of the vertical line through q_i with integer y-coordinate from u_{i+1} to N.[3] Call this set of candidate bend points B_i and let $B = \bigcup_{i=0}^{i=m} B_i$.

2.3.4. The number of vertical strips is in $\Theta(n/\log n)$

We prove here that the number of vertical strips $S_0, \ldots, S_m$ is in $\Theta(n/\log n)$. We first prove that the index u_i of p_{u_i} satisfies $u_{i+1} = u_i + \lceil \log(N - u_i + 1) \rceil$. Recall that $u_0 = 0$ and that the points p_i have coordinates $(-2^i, i)$. By definition $p_{u_{i+1}}$ is the rightmost point of $p_0, \ldots, p_{4n-1}$ that is to the left of q_i (or vertically aligned with q_i). The x-distance between p_{u_i} and q_i is, as shown on Fig. 6, $2^{u_i}(N - u_i)$. Thus the x coordinate of q_i is $-(2^{u_i} + 2^{u_i}(N - u_i))$. By definition of $p_{u_{i+1}}$ we have $2^{u_{i+1}-1} < 2^{u_i} + 2^{u_i}(N - u_i) \leqslant 2^{u_{i+1}}$. Thus $u_{i+1} = u_i + \lceil \log(N - u_i + 1) \rceil$ or equivalently $u_{i+1} = u_i + \lceil \log(4n - u_i) \rceil$.

Since S_i is open on the left side and closed on the right side, the strips are non-intersecting and by construction every element of P (except possibly p_{4n-1}) is contained in one of the strips. Note that u_{i+1} is the size of the intersection of P with $S_0 \cup \cdots \cup S_i$ and so $u_{i+1} - u_i$ is the size of $P \cap S_i$. We have thus established that each S_i contains $\lceil \log(4n - u_i) \rceil$ points of P. In fact, S_i contains the $\lceil \log(4n - u_i) \rceil$ rightmost vertices remaining in P after having removed the u_i rightmost of its vertices – that is, those in $S_0 \cup \cdots \cup S_{i-1}$. Moreover, m is such that P minus the points in $S_0 \cup \cdots \cup S_m$ contains at most one point (since two points are sufficient for defining a strip). It follows that m is the number of iterations (over i) of the process of removing iteratively from a set K (K is initially P) of size $4n$, $\lceil \log(|K|) \rceil$ elements until it is of size at most 1.

So, define, for every $k \geqslant 1$, $T(k)$ to be the number of iterations required to make a set K of size k at most 1 by repeatedly removing $\lceil \log(|K|) \rceil$ of its elements. We claim that $T(k) = T(k/2) + \Theta(k/\log k)$. To see this, note that as long as we have removed fewer than $k/2$ elements of K, we have that $\lceil \log(k) \rceil \geqslant \lceil \log(|K|) \rceil \geqslant \lceil \log(k/2) \rceil = \lceil \log(k) \rceil - 1$. In other words, as long as $|K| \geqslant k/2$, an iteration removes at least $\lceil \log(k) \rceil - 1$ elements from K. Thus, the number of iterations required to make $|K| < k/2$ is at most $\frac{k/2}{\lceil \log(k) \rceil - 1}$, or $\Theta(k/\log(k))$, and so $T(k) = T(k/2) + \Theta(k/\log k)$. The Master theorem then yields that $T(k) = \Theta(k/\log k)$, which establishes that the number of vertical strips created is $\Theta(n/\log n)$.

2.3.5. The number of candidate bend points in every strip S_i is in $\Theta(n)$

We now prove that for each $i = 0, \ldots, m$, $|B_i|$ is in $\Theta(n)$. The line $p_i p_{i+1}$ has equation $y = -2^{-i}x + i - 1$ and intersects the line $y = N$ at $x = -2^i[N - i + 1]$. The line $x = -2^i[N - i + 1]$ intersects the line $p_j p_{j+1}$ (which has equation $y = -2^{-j}x + j - 1$) at $y = (N - i + 1)/2^{j-i} + j - 1$. Thus, on the line $p_j p_{j+1}$, we place $(N - i + 1)/2^{j-i} + j - 1 - j = (N - i + 1)/2^{j-i} - 1 > 0$ candidate bend points. How many bend points will this yield in total for strip S_i? We have some number, call it $k + 1$, of these line segments $p_j p_{j+1}$, starting with $j = i$, giving the sum $\sum_{j=i}^{j=i+k}[(N - i + 1)/2^{j-i} - 1] < \sum_{j=i}^{j=i+k}(N - i + 1)/2^{j-i} < \sum_{j=i}^{j=\infty}(N - i + 1)/2^{j-i} = \sum_{j'=0}^{j'=\infty}(N - i + 1)/2^{j'} = 2(N - i + 1) = O(n)$. Adding the linear number of candidate bend points on the vertical line through q_i results in B_i having size in $\Theta(n)$.

2.3.6. One-bend drawing of Γ' with vertices in P and bend points in B

Now we show that Γ' can be drawn with at most one bend per edge such that its vertices are in P and its bend points are in B. The construction is the same as the one described above with $\Theta(n^2)$ candidate bend points except for the x-coordinates of the bend points that are used. In particular, vertices v_i are still mapped to the p_i (except that the dummy vertices in Γ' are not actually drawn), and an edge $v_i v_j$ completely in the bottom page of Γ' is drawn as the straight line segment $p_i p_j$. As before, an edge $v_i v_j$ that is partially in the top page of Γ' is drawn with a bend point whose height is the same as before, and denoted $h(v_i v_j)$. Note that it is still the case that at most one bend point on any bend line is used. Contrary to the previous construction, the bend point of an edge $v_i v_j$ (with v_i left of v_j) is chosen in B as follows. Let S_k be the vertical strip that contains p_j. The candidate bend point that we choose for edge $v_i v_j$ is the one that lies just to the right of the segment $L_{k,j}$ (the part of the ray from p_j through p_{j+1} that lies in S_k) if that segment extends to height $h(v_i v_j)$; otherwise, the bend point is chosen on the vertical left side of S_k (at height $h(v_i v_j)$).

---

[3] We actually place these bend points infinitesimally close to the right of the vertical line through q_i, only to ensure in the following arguments that these points belong to S_i (which is open on the left).

To complete the proof, it suffices to show that no two edges of Γ' have drawings whose one-bend polylines intersect (except possibly at their endpoints). As mentioned earlier, this proof is very similar to that in [7] and we do not duplicate these arguments here. Instead, we argue that we can move the bend points used in the previous construction (having $\Theta(n^2)$ candidate bend points) to locations in our $\Theta(n^2/\log n)$ point-set B without introducing any crossings. We obtain our drawing on the $\Theta(n^2/\log n)$ point-set from the drawing on the $\Theta(n^2)$ point-set by moving each bend point to the left (on the same bend line) until it reaches its prescribed location.

Consider an edge e whose left and right endpoints are p_i and p_k, respectively, and whose bend point b lies at the height of p_j (and thus $i > j > k$); see Fig. 7. Let b_0 be the initial location of the bend point in the drawing on the $\Theta(n^2)$ point-set, and b_1 be its final location in the drawing on the $\Theta(n^2/\log n)$ point-set. We first argue that when b moves on its bend line from b_0 to b_1, the edge e never intersects any vertex p_ℓ, $\ell \neq i, k$.

Indeed, first observe that by the definition of b_1 (see Fig. 6), segment $p_k b$ does not intersect any vertex other than p_k for any b between b_0 and b_1. Second, segment $p_i b$ does not intersect any vertex other than p_i because, by definition of the points $p_0, \ldots, p_{4n-1}$, segment $p_i b$ intersects segment $p_j p_{j+1}$ (see Fig. 7 and [7, Lemma 6]), thus the line $p_i b$ leaves all the vertices $p_{i-1}, \ldots, p_{j+1}$ strictly above it and all the other vertices (distinct from p_i) strictly below it (for any position of b at the height of p_j, strictly to the right of p_j and to the left of p_0).

Hence, when the bend point of an edge e moves between b_0 and b_1, the edge e does not intersect any vertex (except its endpoints). Observe that if only one edge e moves at a time, its bend point b cannot intersect another edge e' before edge e intersects the bend point of e'; indeed, no two bend points lie at the same height and, as b moves to the left, edge e remains a concave chain of two segments having negative slopes. Thus, it only remains to prove that, if only one edge e moves at a time, it does not intersect any other bend point.

First, observe that, when b moves from b_0 to b_1, the left segment $p_i b$ of edge e intersects no other bend point. Indeed, there is no other bend point at the height of b, and since segment $p_i b$ intersects the segment $p_j p_{j+1}$ (see Fig. 7), the horizontal rays from the p_ℓ, $\ell > j$, and directed to the right (rays which support the bend points above b) do not intersect segment $p_i b$.

It thus remains to prove that, when b moves from b_0 to b_1, the right segment $b p_k$ of edge e intersects no other bend point. Note first that the segment $b p_k$ remains during the motion inside the vertical slab S_u that contains p_k, thus segment $b p_k$ cannot intersect any bend point outside of S_u. To prove that $b p_k$ intersects no bend point inside S_u, we consider the motions of the edges in the right order, that is the increasing order of the height of their bend points. Then, by construction of the $\Theta(n^2/\log n)$ candidate bend points, the edge $b p_k$ cannot intersect any other bend point. Indeed, it may only intersect the bend points in S_u that are below b (and left of p_k), and these are either on the vertical line bounding S_u on its left, or below the line $p_k b_1$. Hence, by considering the motions of the bend points in the given order, the motions do not create any intersection, which completes the proof. □

3. Biconvex point-sets

Any point-set in general position supports the class of outerplanar graphs [5]. Indeed a point-set in convex position supports exactly the class of outerplanar graphs, and no other planar graphs. Motivated by this insight we now consider the class of planar graphs that are supported by a point-set in which $n/2$ points are on one convex curve and the remainder are on another convex curve – in biconvex position. Clearly outerplanar graphs can be supported by this point-set and efficient algorithms such as that developed by Bose [9] exist. We show that any $(n/2, n/2)$ biconvex point-set is universal for a subclass of the series-parallel graphs (Theorem 8) and thus establish Theorem 1. Since our purpose is to exhibit universal point-sets for classes of planar graphs, the balancing condition is critical and since the number of vertices could be odd, the balancing must allow for one vertex to be placed arbitrarily. Henceforth denote by n the number of vertices of the given graph.

A planar graph G is *biconvex* if there exists a crossing-free straight-line drawing Γ of G with all vertices located on the curves λ_1 and λ_2.

A planar graph G is *balanced biconvex* if it is biconvex with a drawing Γ in which the numbers of vertices on the two curves differ by at most one; more formally if:

- For n even, $n/2$ vertices are on λ_1 and $n/2$ vertices on λ_2 (called *uniform* and denoted as $\Gamma^=$).
- for n odd, either:
  - $\frac{n-1}{2}$ vertices are on λ_1 and $\frac{n+1}{2}$ vertices are on λ_2 (called *top-heavy* and denoted as Γ^+), or
  - $\frac{n+1}{2}$ vertices are on λ_1 and $\frac{n-1}{2}$ vertices are on λ_2 (called *bottom-heavy* and denoted as Γ_+).

It is convenient to be less explicit about the provided point-set and focus on the biconvexity property. The following lemma formalizes that this is sufficient to claim a *universal* biconvex point-set of suitable size, since, intuitively, we can shift any biconvex drawing on one point-set to any other point-set with the same numbers of points on the two curves.

Lemma 7. *If a graph G on n vertices has a balanced biconvex drawing, then every balanced biconvex point-set of size n supports G.*

Proof. A drawing with $n/2$ vertices on each of two biconvex curves specifies a particular embedding of the graph. Let u, v, w be three consecutive vertices on one of the two curves. Then v and its incident edges can be shifted to any location between u and w without creating a crossing and without changing the circular ordering around all vertices – thus preserving the specified embedding. A given drawing can be shifted onto any particular point-set, of appropriate cardinality, by preserving the ordering of the vertices along each curve. □

As a result of Lemma 7, we may shift our attention to drawings on biconvex *curves* since a particular point-set is not required.

3.1. Series-parallel graphs and their decomposition trees

The class of graphs that we intend to demonstrate to be balanced biconvex, is a subclass of series-parallel graphs, whose definition we now recall. Although this definition is stated in terms of a directed graph, it is ultimately the underlying undirected graph that we require.

A *two terminal series-parallel digraph* (also called *TTSP-digraph*) is a planar digraph recursively defined as follows [10,11]:

- A directed edge joining two vertices forms a TTSP-digraph.
- Let G' and G'' be two TTSP-digraphs; the digraph obtained by identifying[4] the sink of G' with the source of G'' (*Series Composition*) is also a TTSP-digraph.
- Let G' and G'' be two TTSP-digraphs; the digraph obtained by identifying the source of G' with the source of G'', and the sink of G' with the sink of G'' (*Parallel Composition*) is also a TTSP-digraph.

A TTSP-digraph has one source and one sink which are called its *poles*. Also, a TTSP-digraph is always acyclic and admits a planar embedding with the poles on the same face.

A TTSP-digraph is a *TTSP lattice* if for every directed edge (u, v), there is no directed path from u to v that does not contain (u, v). Note that a TTSP lattice cannot have multiple edges.

The undirected underlying graph of a TTSP-digraph is called a *two terminal series-parallel graph* or *TTSP-graph* for short; similarly, the undirected underlying graph of a TTSP-lattice is called a *two terminal series-parallel lattice* or *TTSP-lattice* for short. We further shorten these terms in the current paper and refer to them as series-parallel (SP).

Associated with a series-parallel graph is a decomposition tree which identifies the operations required to construct the graph. The proofs of several of our lemmas rely on such a decomposition tree, called an SPQ*-tree.

An SPQ*-tree of a TTSP-graph is a simplification of the definition of SPQ*R-trees of general biconnected graphs [12], or, equivalently, of general *st*-graphs. An SPQ*R-tree is a tree having four types of nodes, *S*-, *P*-, *R*-, and *Q*-nodes, which describes a decomposition of G into its triconnected components; more precisely, an *S*-node represents a series component, a *P*-node represents a parallel component, an *R*-node represents a rigid component (i.e. a component that is a triconnected graph), and each *Q*-node represents a simple path of G. If G is series-parallel, its associated SPQ*R-tree has no *R*-nodes and its structure can be described only in terms of *S*-, *P*-, and *Q*-nodes. Also, since G is a TTSP-graph the description of the decomposition process can be further simplified, as described below.

A *separation pair* of G is a pair of vertices such that the removal of these vertices disconnects G. A *split pair* of G is either a separation pair or a pair of adjacent vertices of G. A *split component* of G with respect to a split pair $\{u, v\}$ is either the edge (u, v) or a maximal subgraph C of G such that C is an uv-graph and $\{u, v\}$ is not a split pair of C.

Let G be a TTSP-graph with source pole u and sink pole v. An SPQ*-tree T of G describes a recursive decomposition of G with respect to its split pairs. Intuitively, T represents a natural way to describe G in terms of its series and parallel compositions.

More formally, T is a rooted tree whose nodes are of three types: S, P, and Q^*. Each node μ of T has an associated TTSP-graph (possibly with multiple edges), called the *skeleton* of μ and denoted by *skeleton*(μ). Tree T is recursively defined according to the following cases:

Chain case: G consists of a simple path from u to v. Then, T consists of a single Q^*-node μ. Graph *skeleton*(μ) is G itself.

Series case: Graph G is not a biconnected graph. Let $u_2, \ldots, u_k$ ($k \geqslant 2$) be the cut-vertices of G of degree 3 or more. Since G is planarly biconnectible, each cut-vertex u_i ($i = 2, \ldots, k$) is contained in exactly two connected components G_i and G_{i-1}; also, u is in G_1 and v is in G_k. Each G_i is a TTSP-graph with poles u_i, u_{i+1} ($i = 1, \ldots, k$), where $u_1 = u$, and $u_{k+1} = v$. Then, the root of T is an S-node μ. The *skeleton*(μ) consists of the chain $e_1, \ldots, e_k$, where $e_i = (u_i, u_{i+1})$ (for $i = 1, \ldots, k$). Node μ has children $v_1, \ldots, v_k$, where v_i is the root of the SPQ*-tree T_i of G_i ($i = 1, \ldots, k$). Graph G_i is called the *pertinent graph* of v_i, and edge e_i is called the *virtual edge* of v_i in *skeleton*(μ).

Parallel case: Graph G is a biconnected graph with at least two split components with respect to the split pair $\{u, v\}$. Denote these split components $G_1, \ldots, G_k$ ($k \geqslant 2$). Each G_i ($i = 1, \ldots, k$) is a TTSP-graph with poles u and v. Then, the root of T is a P-node μ. The graph *skeleton*(μ) consists of a bundle of parallel edges e_i from u to v ($i = 1, \ldots, k$).

---

[4] I.e. coalescing.

Node μ has children $\nu_1, \ldots, \nu_k$, where ν_i is the root of the SPQ*-tree T_i of G_i ($i = 1, \ldots, k$). Graph G_i is called the *pertinent graph* of ν_i, and edge e_i is called the *virtual edge* of ν_i in *skeleton*(μ).

3.2. 3SP lattices

A series-parallel graph in which every vertex is of maximum-degree-3 is denoted as 3SP. It is the class of 3SP lattices that we will show to be balanced biconvex. We distinguish between two critical cases. If both the source and sink of a 3SP lattice have degree $\leqslant 2$ then the graph is called *thin* and otherwise (i.e. if either pole has degree 3) it is called *thick*.

There are several simple properties of the decomposition tree T associated with a given 3SP lattice G:

- The parent of an S-node of T must be a P-node.
- A P-node cannot have two P children[5] (maximum-degree 3 constraint would be violated).
- An S-node can have an arbitrary number of children, however no two consecutive children can be P-nodes (maximum-degree 3 constraint would be violated).
- If G is biconnected then the root of T must be a P-node.
- If G is not biconnected then the root of T must be either an S- or Q^*-node.

Further constraints on the decomposition tree will be exploited for special cases, for example if G is thin.

Our construction is recursive and attempts to contain the drawing of the SP lattice in a box spanning the biconvex curves with a balanced number of vertices on each curve and with s and t forming a diagonal of the box. Unfortunately, such a strong invariant cannot be maintained and slightly weaker conditions must be carefully considered.

A series-parallel digraph with poles s and t is *bottom-cornered* if it is balanced biconvex with a drawing $\Gamma^=$ (n even) or Γ_+ (n odd) such that:

1. There exists a box (i.e. a convex quadrilateral) $B(s, t)$ with s on λ_1 and t on λ_2, $\overline{st}$ forms one diagonal of B, and the other diagonal has one corner on λ_1 and one on λ_2, and
2. The entire drawing lies inside B.

See Fig. 14 for an example. Similarly, a series-parallel digraph with poles s and t is *top-cornered* if it is balanced biconvex with a drawing $\Gamma^=$ (n even), or Γ^+ (n odd) such that conditions 1 and 2 hold.

Finally, if a series-parallel graph is both top-cornered and bottom-cornered, it is called *double-cornered* – i.e. if n is odd, there exist two drawings Γ^+ and Γ_+ both of which satisfy conditions 1 and 2. See Fig. 10 for example.

In some situations, only weaker conditions on the drawings of a series-parallel graph can be maintained, in which one of t or s is contained strictly inside a box rather than on the diagonal forming the box:

1′. There exists a box $B(s, x)$ with s on λ_1 and x on λ_2, $\overline{sx}$ forms one diagonal of $B(s, x)$, and the other diagonal has one corner on λ_1 and one on λ_2 and t is on λ_2 inside $B(s, x)$.
1″. There exists a box $B(x, t)$ with x on λ_1 and t on λ_2, $\overline{xt}$ forms one diagonal of $B(x, t)$, and the other diagonal has one corner on λ_1 and one on λ_2 and s is on λ_1 inside $B(x, t)$.

A series-parallel graph with source s and sink t is *sink-covered* if it is balanced biconvex and conditions 1′ and 2 hold (see Fig. 18 for example); similarly, if conditions 1″ and 2 hold, then the graph is *source-covered*.

Theorem 8. *The class of 3SP lattices is balanced biconvex.*

It is the class of 3SP lattices that we now show to be balanced biconvex. There are several cases to consider depending on whether the graph is biconnected or not, and whether the graph is thin or thick. Our proof is recursive in nature – interior components are replaced by appropriate balanced boxes. Lemmas 9–15 distinguish and organize these cases and Fig. 8 provides a simple example of each case, the type of drawing obtained, and the prerequisite lemmas used in the proof.

The following invariant is maintained in Lemmas 9, 10 and 11 and is used inductively.

Invariant I: Let T be the decomposition tree. For all nodes μ of T with poles s_μ and t_μ, and for every edge (u, v) of G_μ such that $u \neq s_\mu$ and $v \neq t_\mu$, u and v are drawn on opposite curves and there exists a box $B(u, v)$ that is empty except for the edge (u, v).

Fig. 9 provides an example of the technique used. In this example, the 3SP lattice with poles s_1 and t_3 is not biconnected and has one (global) pole of degree 3, and thus Lemma 15 will apply. Since this graph consists of a series of 3 component SP lattices, with poles (s_1, t_1), (t_1, s_3), and (s_3, t_3) Lemmas 10, 9, and 14 respectively are applied. The first two SP lattices can be drawn double-cornered, however the third is bottom-half-cornered.

---

[5] Furthermore, only at the topmost level can a P-node have even a single child that is a P-node.
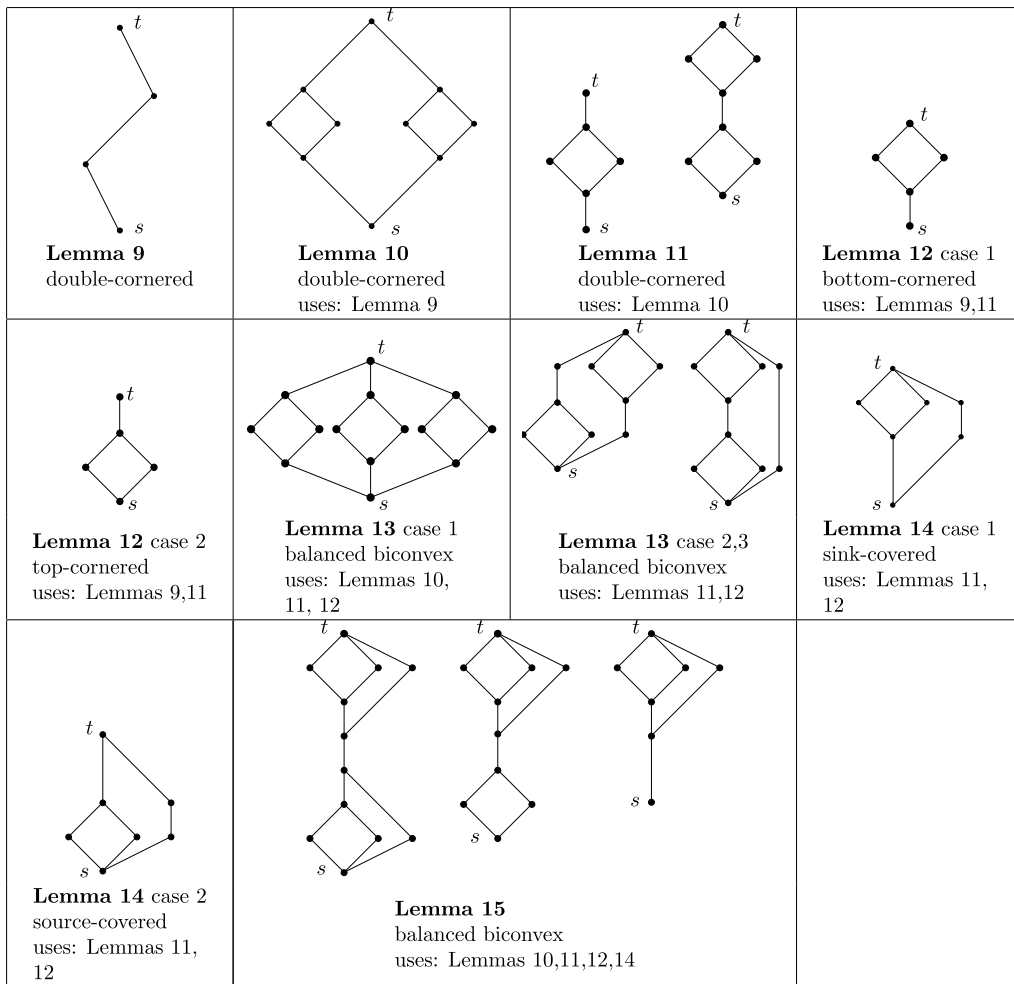
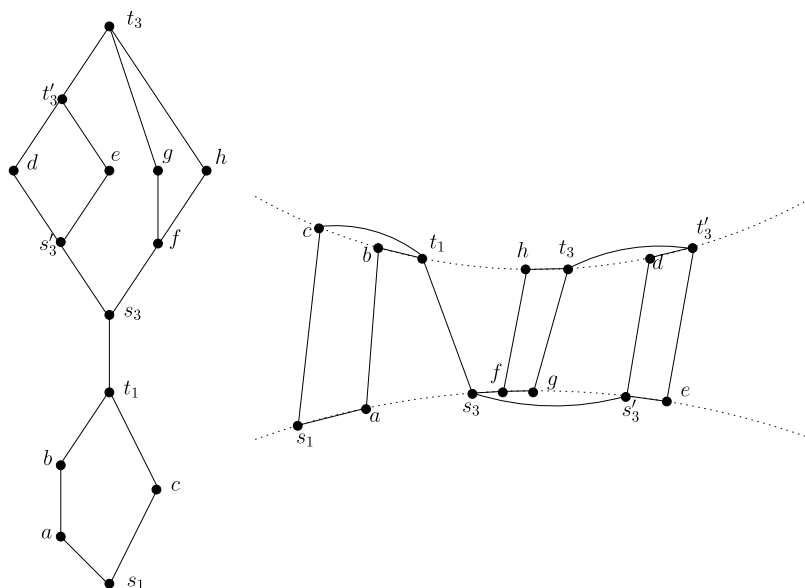**Fig. 8.** Roadmap of the various cases.

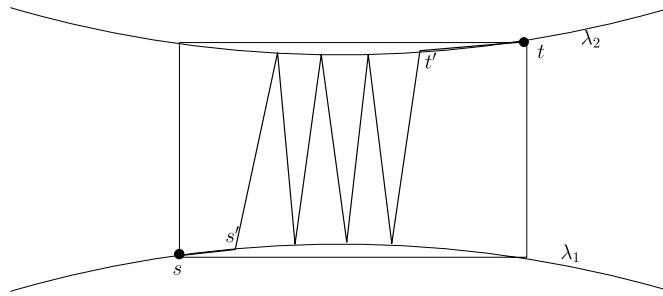**Fig. 9.** Example construction (3 edges are drawn curved for clarity).

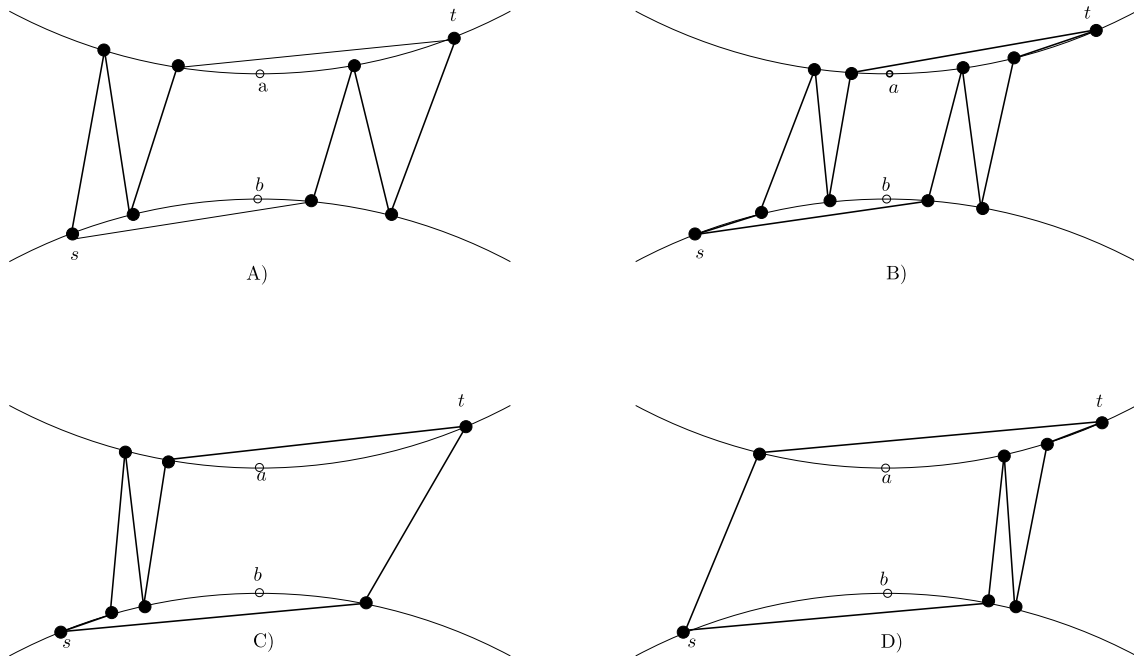**Fig. 10.** (Lemma 9) Paths are double-cornered.

Fig. 11. (Lemma 10) Base case: 2 chains from s to t; (A) odd, odd $\Rightarrow \Gamma^=$; (B) even, even $\Rightarrow \Gamma^=$; (C) and (D) even, odd $\Rightarrow \Gamma^+$, or Γ_+.

Lemma 9. *A simple path consisting of $n \geqslant 2$ vertices from s to t is double-cornered.*

Proof. Refer to Fig. 10. Let the neighbor of s be s' and the neighbor of t be t'. If n is even, the path can alternately place vertices on λ_1 and λ_2, as in Fig. 10. If n is odd, then either s' or t' can be relocated to the opposite curve to produce top-heavy or bottom-heavy drawings. □

3.3. Thin 3SP lattices

This subsection considers those lemmas used for subcases that are thin.

Lemma 10. *Let G be a biconnected thin 3SP lattice. Then G is double-cornered.*

Proof. Consider the decomposition tree T of G. Since G is biconnected, the root of T is a P-node. The lemma is proven by induction on the number of P-nodes in T and invariant I is maintained throughout.

Base case: The simplest form of a biconnected thin 3SP lattice consists of two chains from s to t, i.e. the decomposition tree is a single P-node with two Q^* children. Lemma 9 is applied carefully on each chain depending on the parity of the number of vertices on each chain to obtain double-cornered drawings – the cases are shown in Fig. 11.

Let l and r denote the number of vertices on the left and right chains respectively, excluding s and t. Since G is a lattice, $l, r \geqslant 1$. We choose a point on λ_1 for s and a point on λ_2 for t. Box $B(s, t)$ is split into two sub-boxes: $B(s, a)$ and $B(b, t)$, where a is a point on λ_2 left of t and b a point on λ_1 right of s. If l and r are both odd, then n is even and a uniform
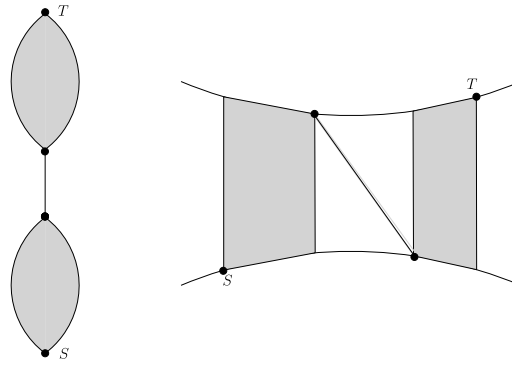
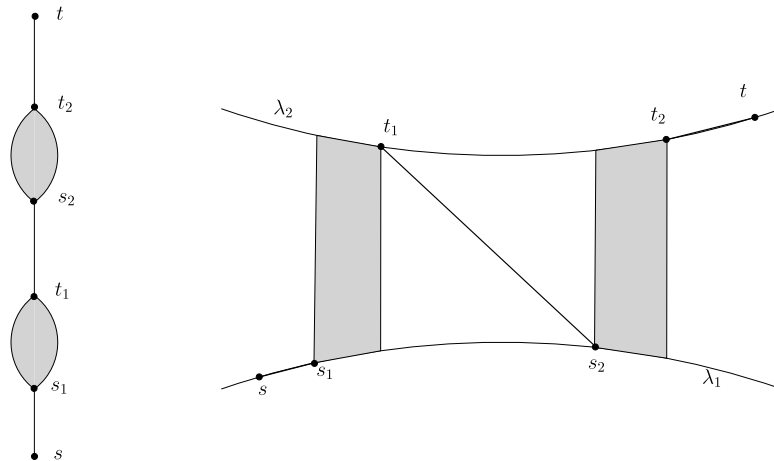**Fig. 12.** (Lemma 11) Both *s* and *t* have degree 2.

Fig. 13. (Lemma 11) Both *s* and *t* have degree 1.

drawing $\Gamma^=$ is produced with the left chain in box $B(s,a)$ and the right chain in $B(b,t)$ and each box is uniform. If l and r are both even, then n is even and a uniform drawing $\Gamma^=$ is produced with the left chain in box $B(s,a)$ bottom-heavy, and the right chain in $B(b,t)$ top-heavy. In the final case, one of l and r is odd and the other is even, and thus n is odd. A bottom-heavy drawing is produced by drawing the even chain in the box $B(s,a)$ bottom-heavy, and the odd chain in $B(b,t)$ uniform. A top-heavy drawing uses $B(s,a)$ for the odd chain drawn uniform, and $B(b,t)$ for the even chain drawn top-heavy. Thus, G is double-cornered.

Inductive case: Assume by induction that every biconnected, thin 3SP lattice whose decomposition tree has less than k P-nodes is double-cornered and respects invariant I and let G be a biconnected, thin 3SP lattice whose decomposition tree T has k P-nodes.

Visit T from the leaves to the root and let ν be the first encountered P-node. All children of ν are Q^*-nodes. Let μ be the parent of ν and let ρ be the parent of μ in T. Note that μ is an S-node and ρ is a P-node. Furthermore, neither $s_\nu \equiv s_\mu$ nor $t_\nu \equiv t_\mu$, since G is a biconnected, thin 3SP graph. Replace G_ν with an edge (s_ν, t_ν) which we call a *virtual edge*, and let G' be the resulting biconnected, thin 3SP lattice with corresponding decomposition tree T'. Since T' has fewer than k P-nodes, G' is double-cornered and its drawing, Γ', satisfies invariant I. Consider the box $B(s_\nu, t_\nu)$ in Γ' and the pertinent graph G_ν of ν in T. Applying the base case, G_ν can be double-cornered in $B(s_\nu, t_\nu)$, thus providing a double-cornered drawing for G. □

We now extend the previous lemma by considering thin 3SP lattices that are not biconnected.

Lemma 11. *Let G be a thin 3SP lattice with source s and sink t. If either $\deg(s) = \deg(t) = 1$ or $\deg(s) = \deg(t) = 2$ then G is double-cornered.*

Proof. Case 1 (both s and t have degree 2): Refer to Fig. 12. If G is biconnected, then the previous lemma applies, so assume G is not biconnected, with decomposition tree T. Let μ be the root of T with children $\nu_1, \ldots, \nu_k$ in left-to-right order. Note that μ is an S-node and both ν_1 and ν_k are P-nodes. Also, if ν_j and ν_l are two P-nodes, there exists a Q^*-node ν_x with $j < x < l$, i.e. $\nu_1, \ldots, \nu_k$ is an alternating sequence of P-nodes (odd subscripts) and Q^*-nodes (even subscripts). For each
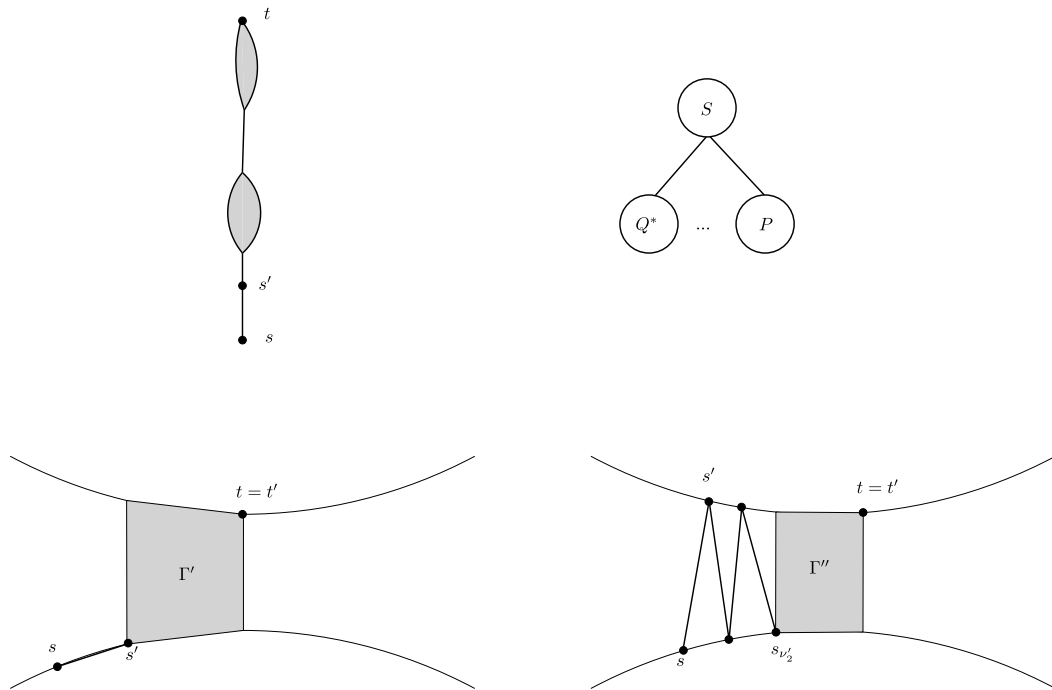
Fig. 14. (Lemma 12) Bottom-cornered.

P-node ν_j, the pertinent graph G_{ν_j} satisfies Lemma 10 and thus is double-cornered. Each ν_j is drawn in a box between the box of $G_{\nu_{j-2}}$ and the box of $G_{\nu_{j+2}}$.

For each Q^*-node ν_i, consider the box B_i defined by the diagonally opposite corners $t_{\nu_{i-1}}$ and $s_{\nu_{i+1}}$. Draw G_{ν_i} as described in Lemma 9 and observe that the resulting drawing is double-cornered.

Case 2 (both s and t have degree 1): Refer to Fig. 13. Both the leftmost child ν_1 and rightmost child ν_k of μ are Q^*-nodes. Consider the subgraph G' of G obtained by deleting the pertinent graphs G_{ν_1} and G_{ν_k}. Either G' satisfies Lemma 10 or the previous case of this proof and thus G' can be double-cornered. Let Γ' be the corresponding balanced biconvex drawing. We choose a point s on the curve opposite to that of s_{ν_1}, and a point t on the curve opposite to that of t_{ν_k}, and so that the box defined by s and t contains Γ'. We now draw G_{ν_1} in the box $B(s, t_{\nu_1})$ and G_{ν_k} in the box $B(s_{\nu_k}, t)$ by using Lemma 9. The resulting drawing is double-cornered. □

Lemma 12. *Let G be a thin 3SP lattice with source s and sink t. If $\deg(s) = 1$ and $\deg(t) = 2$ (respectively $\deg(s) = 2$ and $\deg(t) = 1$) then G is bottom-cornered (resp. top-cornered).*

Proof. First case: $\deg(s) = 1$ and $\deg(t) = 2$. Refer to Fig. 14. Let T be the decomposition tree of G. Let μ be the root of T with children $\nu_1, \ldots, \nu_k$ in left-to-right order. Note that μ is an S-node and that ν_1 is a Q^*-node and ν_k is a P-node. Let s' be the (single) neighbor of s. Remove edge (s, s') from G and call the resulting thin 3SP lattice G'. There are now two cases to examine. Assume first that both the source s' and the sink t' of G' are of degree 2. Then G' satisfies the condition of Lemma 11 and hence is double-cornered; let Γ' be the corresponding drawing. Assume without loss of generality that s' is the leftmost vertex on the bottom curve λ_1. We compute a drawing Γ of G by adding a vertex s left of s' on λ_1 and adding the edge (s, s'). This drawing is boxed but bottom-heavy since s is on the same curve as s'. Thus Γ is bottom-cornered.

Assume now that s' has degree 1. Let the decomposition tree of G' be T' with root μ'; let the children of μ' be $\nu_1', \ldots, \nu_k'$. Recall that ν_1' is a Q^*-node. Delete $G_{\nu_1'}$ from G' and call the resulting thin 3SP lattice G''. By Lemma 11 G'' is double-cornered and has a drawing Γ''. Assume $s_{\nu_2'}$ is on λ_1. Choose a point s' on λ_2 such that $B(s', s_{\nu_2'})$ does not intersect Γ''. Draw $G_{\nu_1'}$ in $B(s', s_{\nu_2'})$ via Lemma 9. Let Γ' be the resulting drawing and observe that Γ' is uniform but not boxed since s' and t' are on the same curve. We draw s at a point on λ_1 such that s is left of any other vertex of Γ' and add edge $\overline{ss'}$. Since Γ' is uniform, Γ is bottom-cornered.

For the second case, the roles of s and t can be reversed in the above proof to construct a drawing that is top-cornered. □
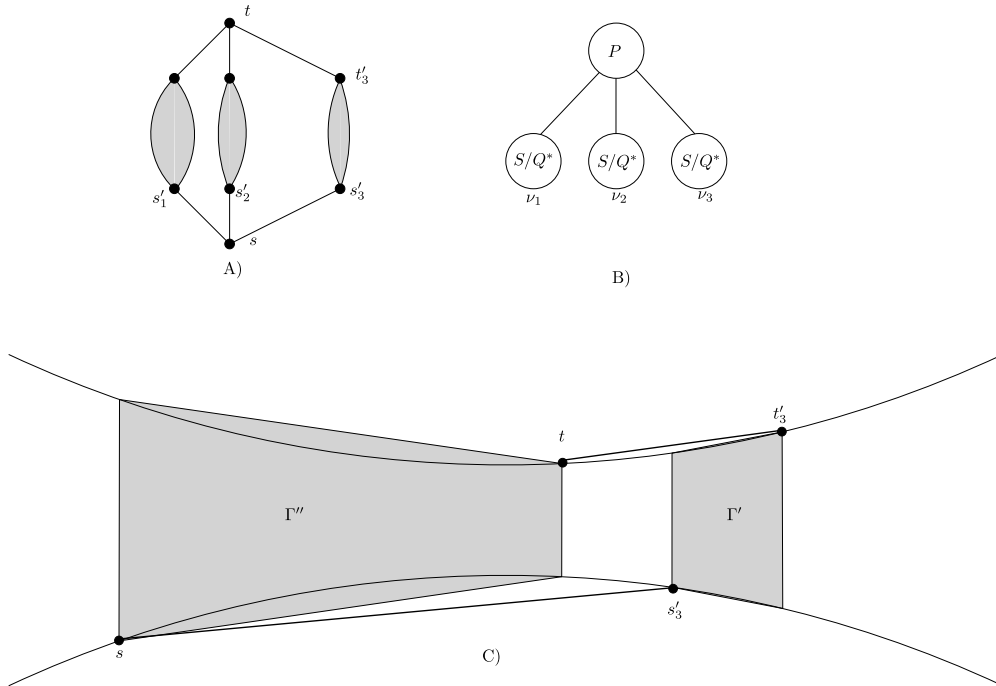
Fig. 15. (Lemma 13 case 1) (A) Sketch of graph; (B) Decomposition tree; (C) Drawing.

3.4. Thick 3SP lattices

The next sequence of lemmas pertains to the cases when the global poles have degree 3. The drawings obtained rely on the previous lemmas and are balanced biconvex, but may not be double-cornered. We start with the cases when G is biconnected.

Lemma 13. *Let G be a biconnected 3SP lattice with source s and sink t. If $\deg(s) = \deg(t) = 3$ then G is balanced biconvex.*

Proof. We partition this situation into three cases. Let T be the decomposition tree of G and let μ be the root of T.

Case 1: G consists of three series components (S or Q^*) combined in parallel. Note that μ is thus a P-node with exactly three children each of which is an S-node or a Q^*-node. Let ν_1, ν_2, and ν_3 be the three children of μ in left-to-right order. Observe that for each ν_i ($i = 1, 2, 3$) both the leftmost and rightmost child of ν_i is a Q^*-node if ν_i is a S-node. Let s_3' (resp. t_3') be the neighbor of s (resp. t) in G_{ν_3}. Let G' be the subgraph of G_{ν_3} obtained by deleting vertices s and t from G_{ν_3}. Graph G' is a thin 3SP lattice that satisfies the hypothesis of Lemmas 11, or 12. Let G'' be the subgraph of G obtained by deleting all vertices of G'. Graph G'' is a biconnected thin 3SP lattice that satisfies the conditions of Lemma 10. We now place 4 points on λ_1 and λ_2 as shown in Fig. 15. Via Lemma 10, we box G'' into $B(s, t)$ and using one of Lemmas 11, or 12, we box G' into $B(s_3', t_3')$ and add the segments corresponding to the edges (s, s_3') and (t, t_3'). Let Γ' be the drawing of G' and Γ'' be the drawing of G''. If G' was boxed into $B(s_3', t_3')$ by using Lemma 12 case 1, then Γ' is bottom-heavy. Let n'' be the number of vertices of G''. If n'' is even, then Γ is bottom-heavy. If n'' is odd, then by Lemma 10, we can make Γ'' top-heavy and so Γ is uniform. A similar argument applies if Lemma 12 case 2 is used to compute Γ', in which case Γ is either top-heavy or uniform. Finally, if Lemma 11 applies, then Γ' is double-cornered and hence Γ is uniform.

There are two further forms. In both forms, s is the pole of some P-node, as is t.

Case 2: The P-nodes are on opposite sides of the two chains from s to t. See Fig. 16. Here μ is a P-node with children ν_1 and ν_2 in left-to-right order. Also, the leftmost child of ν_1 is a P-node and the rightmost child is a Q^*-node. Symmetrically, the leftmost child of ν_2 is a Q^*-node and its rightmost child is a P-node.

Let G' be the subgraph of G_{ν_1} obtained by deleting t from G_{ν_1}, and let G'' be the subgraph of G_{ν_2} obtained by deleting s from G_{ν_2}. Let t' be the sink of G', and s'' be the source of G''. Observe that G' satisfies the hypothesis of either Lemma 11 or Lemma 12 case 2; G'' satisfies the hypothesis of either Lemma 11 or Lemma 12 case 1. We construct a drawing Γ of G as shown in Fig. 16C, where Γ' and Γ'' represent the drawings of G' and G'' respectively. Let n' (resp. n'') be the number of vertices of G' (resp. G''). If at least one of n' or n'' is an even integer, then by construction, Γ is either uniform, or top-heavy, or bottom-heavy. Assume that both n' and n'' are odd integers and that G' satisfies Lemma 11. We can compute Γ' so that it is top-heavy, while Γ'' will be computed as a bottom-heavy drawing by either Lemma 11 or Lemma 12 case 1. Hence, Γ is uniform. Similarly, if n' and n'' are both odd and G'' satisfies Lemma 11, Γ is uniform. Finally, if G' satisfies
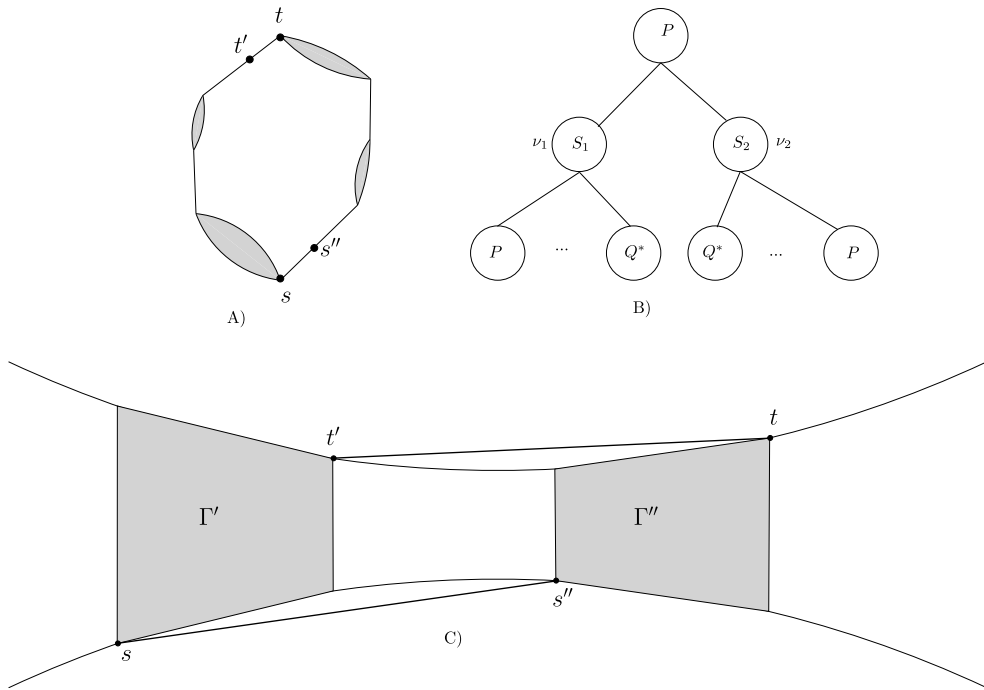
Fig. 16. (Lemma 13 case 2) s and t both have degree 3. (A) Sketch of graph; (B) Decomposition tree; (C) Drawing.
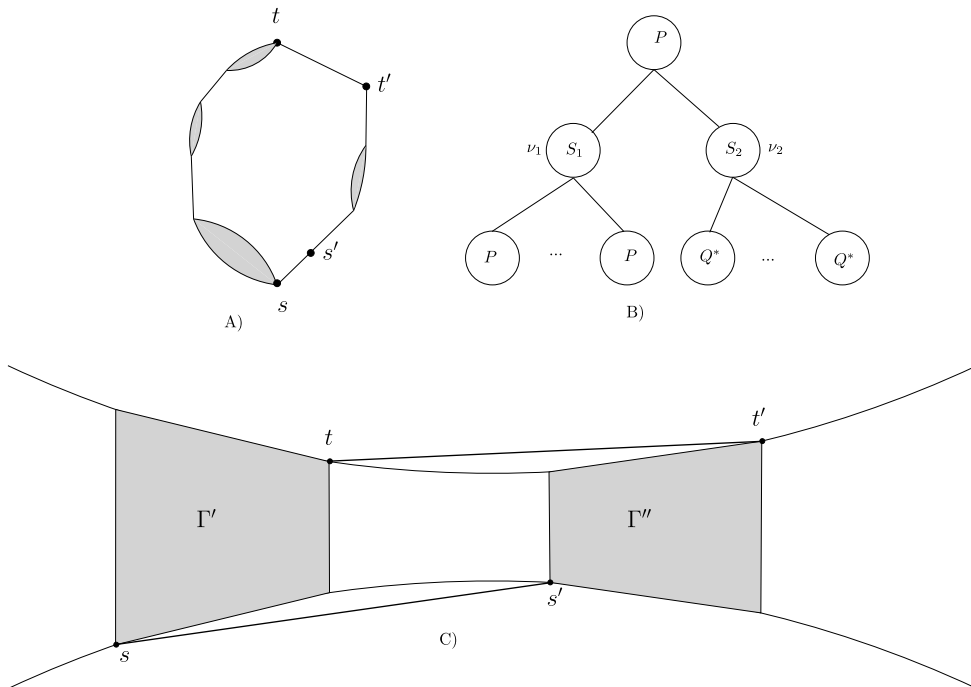

Fig. 17. (Lemma 13 case 3) s and t both have degree 3. (A) Sketch of graph; (B) Decomposition tree; (C) Drawing.

Lemma 12 case 2 and G'' satisfies Lemma 12 case 1, and n' and n'' are both odd, we have that Γ' is top-heavy, Γ'' is bottom-heavy, and thus Γ is uniform.

Case 3: The decomposition tree has one chain that starts and ends with Q^*-nodes. See Fig. 17. Suppose ν_1 is the node of the decomposition tree that starts and finishes with a P-node, and ν_2 starts and finishes with Q^*-nodes. Let G' be the subgraph G_{ν_1} and G'' be the subgraph of G_{ν_2} obtained by deleting s and t from G_{ν_2}. Then G' satisfies the conditions of
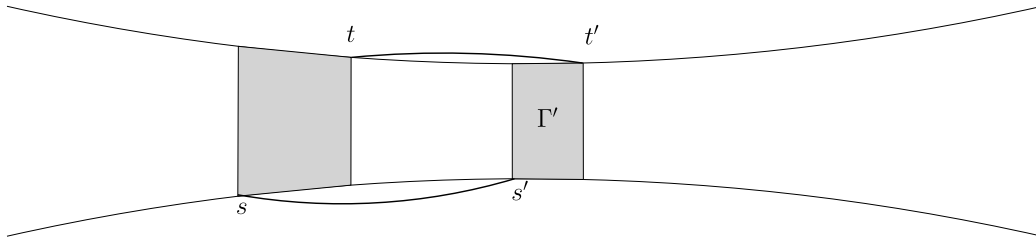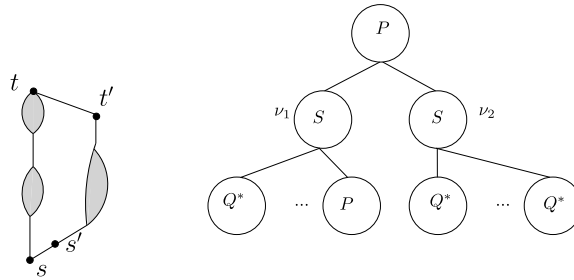
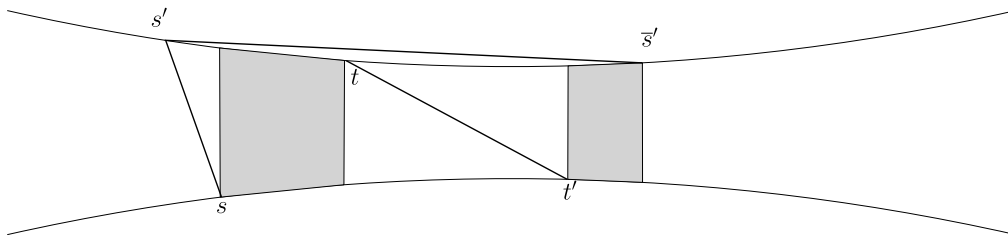**Fig. 18.** (Lemma 14) Sketch of graph; Decomposition tree; Drawing.

Fig. 19. (Lemma 14) Flip and wind.

Lemma 11 case 1, and can be drawn double-cornered as Γ'. G'' satisfies Lemma 11, or 12; its drawing, Γ'' can be drawn and the edges $\overline{ss'}$ and $\overline{t't}$ can be added. Since Γ' is double-cornered, the balancing conditions are easily satisfied. □

Lemma 14. *Let G be a biconnected 3SP lattice with source s and sink t. If $\deg(s) = 2$ and $\deg(t) = 3$ (respectively $\deg(s) = 3$ and $\deg(t) = 2$) then G is sink-covered (resp. source-covered).*

Proof. Case 1: $\deg(s) = 2$ and $\deg(t) = 3$. Let T be the decomposition tree of G and let μ be the root of T. Thus μ is a P-node with exactly two children ν_1, and ν_2 in left-to-right order. Note that at most one of them can be a Q^*-node and that exactly one of them has a P-node as its rightmost child (namely the P-node having t as one of its poles) – assume without loss of generality the latter is ν_1. Let G' be the subgraph of G_{ν_2} obtained by deleting s and t from G_{ν_2}, and let s' and t' be the source and sink of G'. If G' satisfies the hypothesis of Lemma 11 or 12 case 2, we construct a sink-covered drawing Γ of G as follows. Choose 4 points s, t, s', t' on λ_1 and λ_2 as shown in Fig. 18. Via Lemma 12, we draw G_{ν_1} in $B(s,t)$, and by using either Lemma 11 or 12, we draw G' in $B(s',t')$. Finally, we add the segments corresponding to the edges (s,s') and (t,t'). The resulting drawing Γ is sink-covered by construction – t is inside the box $B(s,t')$ and since the drawing of G' is either uniform or top-heavy, while the drawing of G_{ν_1} is either uniform or bottom-heavy, the total drawing is not unbalanced.

Consider now the case in which G' satisfies the hypothesis of Lemma 12 case 1. Let n' be the number of vertices of G' and let n_1 be the number of vertices of G_{ν_1}. If either n' or n_1 is an even integer, then a sink-covered drawing Γ of G is constructed as in the previous case; see Fig. 18. Namely, in this case either the drawing of G_{ν_1} or of G' is uniform and thus Γ is either uniform or bottom-heavy.

Otherwise, both n' and n_1 are odd and we construct a uniform drawing Γ of G as follows. Let $\overline{G'}$ be the subgraph of G' obtained by deleting s' from G'. Let $\overline{s'}$ be the source of $\overline{G'}$; observe that the sink of $\overline{G'}$ is t'. Since $\overline{G'}$ has an even number of vertices, it has a uniform drawing $\overline{\Gamma'}$ in a box $B(\overline{s'},t')$ and we define this box as shown in Fig. 19. Finally, we add vertex s' on the top curve and add segments corresponding to the edges (s,s') and $(s',\overline{s'})$ as in Fig. 19. Observe that the drawing of G_{ν_1} is bottom-heavy and the drawing of $\overline{G'}$ is uniform. Since s' is located on the top curve, the drawing Γ is uniform.
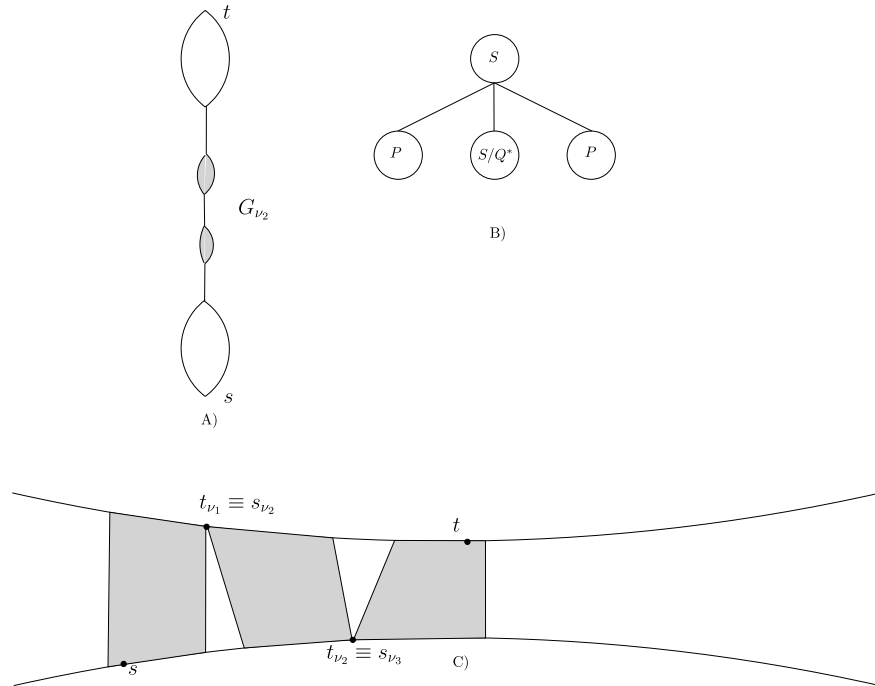
Fig. 20. (Lemma 15) Not biconnected and *s* or *t* has degree 3. Sketch of graph. Decomposition tree. Drawing.
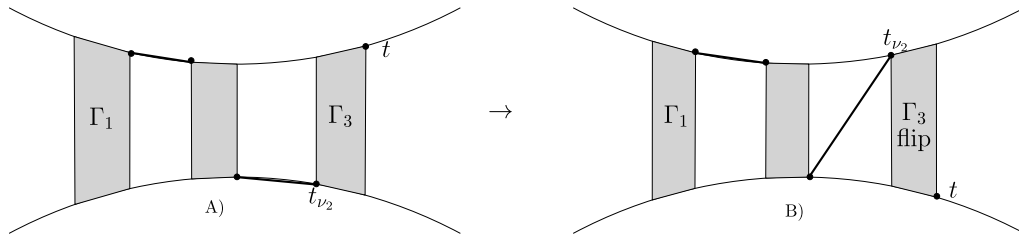

Fig. 21. (Lemma 15) Flip operation.

For the second case, the roles of *s* and *t* can be reversed in the above proof to construct a drawing that is source-covered. □

In the final case, *G* is not biconnected and at least one of the global poles has degree 3.

Lemma 15. *Let G be a 3SP lattice with source s and sink t. If* $\deg(s) = 3$ *or* $\deg(t) = 3$ *then G is balanced biconvex.*

Proof. Refer to Fig. 20. Assume first that neither *s* nor *t* have degree 1. If *G* is biconnected then Lemma 14 or Lemma 13 would apply, so we consider the case that *G* is not biconnected. Let *T* be the decomposition tree of *G* and let μ be the root of *T*. Then μ is an *S*-node and has at least three children. In the simplest case, these three children can be labeled ν_1, ν_2, ν_3 in left-to-right order with ν_1 and ν_3 being *P*-nodes, and ν_2 being a Q^*-node. In general, the first and last child of μ are *P*-nodes, but there is a series of children between them starting and ending with Q^*-nodes. For convenience, we collapse this intermediate series into a single child ν_2 of root μ. A biconvex drawing Γ of *G* is computed as follows. Define three boxes, as in Fig. 20. Draw G_{ν_1} in $B(s_{\nu_1}, t_{\nu_1})$, G_{ν_2} in $B(s_{\nu_2}, t_{\nu_2})$, and G_{ν_3} in $B(s_{\nu_3}, t_{\nu_3})$, by using Lemmas 10 and 14 for G_{ν_1} and G_{ν_3}, and using Lemma 11 for G_{ν_2}. Let n_1 be the number of vertices of G_{ν_1}, n_2 be the number of vertices of G_{ν_2}, and n_3 be the number of vertices of G_{ν_3}. Observe that G_{ν_2} satisfies the hypothesis of Lemma 11 and hence if n_2 is odd, the biconvex drawing of G_{ν_2} inside $B(s_{\nu_2}, t_{\nu_2})$ can be chosen to be top-heavy or bottom-heavy. Hence if n_2 is odd, independent of whether n_1 and n_3 are odd or even, Γ can be computed so that the number of vertices in the top curve differs by at most one from the number of vertices in the bottom curve. If n_2 is even, we distinguish two subcases:
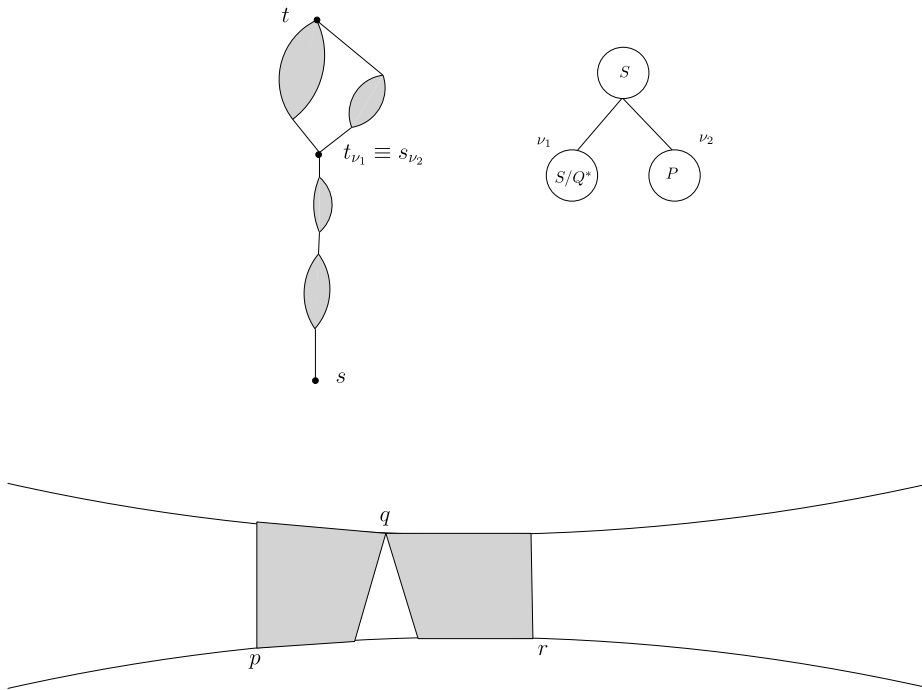
Fig. 22. (Lemma 15) $\deg(s) = 1$, $\deg(t) = 3$. Sketch of graph. Decomposition tree. Drawing.
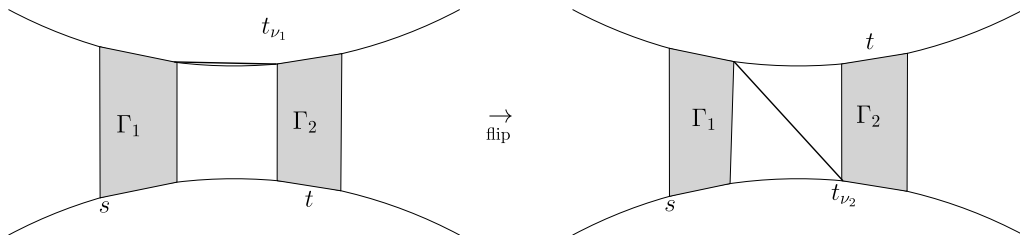

Fig. 23. (Lemma 15) Flip operation.

- Either n_1 or n_3 is even. In this case, either the drawing of G_{ν_1} or of G_{ν_3} is balanced. Since n_2 is even, also the drawing of G_{ν_2} is balanced. As a result the number of vertices of Γ in the top curve differs by at most one from the number of vertices in the bottom curve.
- Both n_1 and n_3 are odd. If both the drawing Γ_1 of G_{ν_1} is source-covered and the drawing Γ_3 of G_{ν_3} is sink-covered (i.e. Γ_1 is computed via Lemma 14 case 2, and Γ_3 via Lemma 14 case 1) it may happen that Γ_1 and Γ_3 are both top-heavy or both bottom-heavy. If this is the case, then we modify Γ as follows. Refer to Fig. 21 where we assume both are bottom-heavy. We flip Γ_3, which produces a top-heavy drawing Γ'_3. The flipping operation is possible because within G_{ν_2}, there is a single edge into t_{ν_2} and Lemma 11 ensures that t_{ν_2} is on a corner of the box containing G_{ν_2}. After the flip the drawing of Γ_{ν_2} is also top-heavy but the drawing Γ_1 remains bottom-heavy, so the drawing Γ is uniform. Note that Γ_2 without the shared poles s_{ν_2} and t_{ν_2} remains balanced. The case where Γ_1 and Γ_3 are both top-heavy is symmetric. Finally, observe that if one of Γ_1 and Γ_3 is top-heavy and the other is bottom-heavy, then Γ is already uniform and no flipping operation is required.

Now assume s has degree 1 and t has degree 3. The root μ of T has in its simplest form two children ν_1 and ν_2 in left-to-right order, such that ν_1 is a Q^*-node, while ν_2 is a P-node. More generally, μ has a series of children starting and finishing with Q^*-nodes followed by a P-node. For convenience, we consider the initial series of children as a single child ν_1, and the final P-node labeled ν_2. We define two boxes as in Fig. 22. We then compute a cornered drawing Γ_1 of G_{ν_1} in box $B(p, q)$ such that $s \equiv p$ and $q \equiv t_{\nu_1}$. We compute a drawing Γ_2 of G_{ν_2} inside $B(q, r)$. Observe that since G_{ν_2} satisfies the hypothesis of Lemma 14 it is sink-covered and thus t is not mapped to r but is contained in the box $B(q, r)$. Since G_{ν_1} satisfies Lemma 11, we compute Γ_1 so that it is either uniform or top-heavy. Let Γ be the resulting drawing. If Γ_1 and Γ_2 are both uniform, then since t_{ν_1} is a common vertex of both drawings, Γ must be bottom-heavy. If Γ_1 (resp. Γ_2) is uniform and Γ_2 (resp. Γ_1) is top-heavy then Γ is necessarily uniform.

If Γ_1 and Γ_2 are both top-heavy then Γ is top-heavy. It remains to consider the case that Γ_1 is uniform and Γ_2 is bottom-heavy. This case is handled with a flip operation as demonstrated in Fig. 23. Flipping Γ_2 makes it top-heavy and the resulting drawing becomes uniform. $\square$

The above lemmas enumerate all possible maximum-degree-3 series-parallel lattices and demonstrate constructively that all such graphs are balanced biconvex, and hence establish Theorem 1. Biconvex point-sets are the only known point-sets of size n that universally support some class of planar graphs other than the outerplanar graphs.

The relevance of the *lattice* constraint in our technique is evident in the base case of Lemma 10. If one of the two chains in that case were the single edge (s, t), then in order to achieve a balanced partition of the vertices, the drawing would necessarily be either sink-covered or source-covered instead of double-cornered. Subsequent lemmas, such as Lemma 11, rely on their subgraphs being double-cornered in order to produce an appropriate drawing. Fig. 20 displays a situation in which the maximum-degree 3 constraint is critical to our construction. In that figure, neither s nor t is on a diagonal of the box containing the drawing. If in addition, there existed a path s, v, t, the path could not be drawn, even though the graph would be a valid 4SP lattice. It is unlikely that the approach taken in this paper can be modified to accommodate the removal of either of these two constraints. We conjecture that neither the class of 3SP *graphs*,[6] nor the class of 4SP lattices is balanced biconvex.

It is clear that the class of maximal planar graphs is not balanced biconvex for $n \geqslant 4$, since in any biconvex drawing, there exists a face of size at least 4.

3.5. Application and remark

An immediate consequence of Theorem 1 concerns the simultaneous embedding of planar graphs. A set of planar graphs $G_1, \ldots, G_k$ ($k \geqslant 2$) each having n vertices has a *simultaneous embedding without mapping* if there exists a set S of n points that supports the straight-line drawing of $G_1, \ldots, G_k$. It is not known whether such a simultaneous embedding exists when $G_1, \ldots, G_k$ are general planar graphs. Braß et al. [13] observed that if G_1 is a planar graph and $G_2, \ldots, G_k$ are outerplanar graphs, then a simultaneous embedding without mapping for $G_1, \ldots, G_k$ exists. The following corollary is a similar observation in this context.

Corollary 16. *Let $G_1, \ldots, G_k$ ($k \geqslant 2$) be a set of 3SP lattices, all having n vertices. There exists a simultaneous embedding without mapping for the set $G_1, \ldots, G_k$.*

3.6. Unbalanced biconvex point-sets

More generally, biconvex drawings may have h vertices on one curve and $n - h$ on the other curve. Any graph that is biconvex drawable (for any value of h) is clearly sub-Hamiltonian, and indeed a stronger condition holds. If the drawing is converted to a book embedding by rotating and translating the vertices on the lower curve, then the resulting book embedding consists of two subgraphs of cycles (one of h vertices and one of $n - h$ vertices) each of which is individually outerplanar (edges are crossing-free on the upper side of the book embedding). And edges between the two outerplanar graphs are on the lower side of the spine and are nested and hence do not cross.

We now show that Theorem 8 is tight in the sense that not every (unbalanced) biconvex point-set is universal for the class of 3SP lattices. We first observe a simple property of any biconvex drawing.

Lemma 17. *If G is a graph with n vertices that is $(k, n - k)$ biconvex drawable, then there exists a set of k vertices in G whose removal results in an outerplanar graph.*

Proof. Consider a $(k, n - k)$ biconvex drawing of G. Removal of the k vertices on one curve, leaves a graph with $n - k$ vertices all on one curve – such a graph is necessarily outerplanar. $\square$

Theorem 18. *For every value of n there exists a 3SP lattice G with n vertices such that in every biconvex drawing of G, there are at least $\lfloor n/7 \rfloor$ vertices on both of the two curves.*

Proof. Consider a biconvex drawing of the diamond graph D in Fig. 24. Since it is not outerplanar, any biconvex drawing of it requires that both curves contain vertices.

Create a chain of $\lfloor n/7 \rfloor$ diamonds and add a path of $n - 7 \cdot \lfloor n/7 \rfloor$ vertices to create a graph G with n vertices that is a 3SP lattice and requires the removal of at least $\lfloor n/7 \rfloor$ vertices to make it outerplanar (since each diamond is independent). Now suppose there exists a biconvex drawing of G in which one of the curves contains fewer than $\lfloor n/7 \rfloor$ vertices. By the
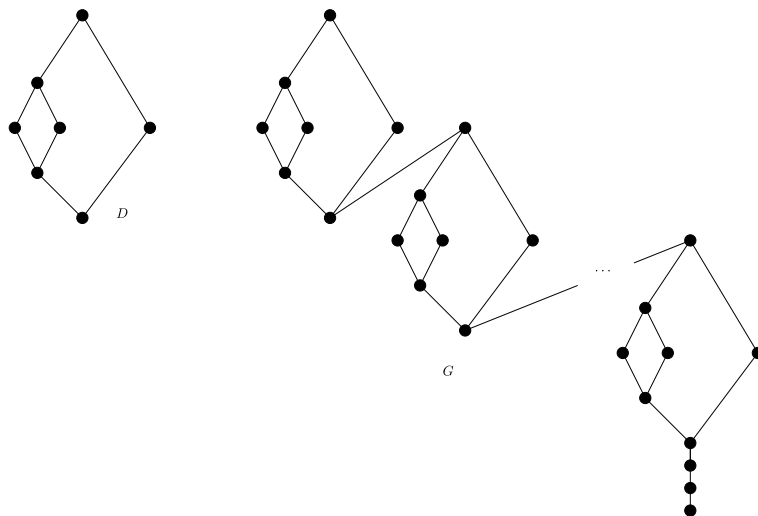
---

[6] Rather than lattices.

Fig. 24. Chain of diamonds.

previous lemma, there then exists some set of fewer than $\lfloor n/7 \rfloor$ vertices whose removal yields an outerplanar graph, which is a contradiction. $\quad\square$

Characterizing and efficiently recognizing those graphs that can be drawn biconvex (balanced or not), remains an interesting open question.

4. Conclusions and open problems

Our main contributions in this paper are stated in Theorems 1 and 2. In the former, we prove that any balanced biconvex point-set supports the straight-line drawing of any 3SP lattice, and in the latter, we supply universal point-sets for drawings of any planar graph with a small number of bends per edge. Since these results pertain to universal point-sets, they trivially imply corollaries in the context of simultaneous graph drawing (without mapping), since any number of graphs can be simultaneously drawn on a universal point-set.

There remain many open problems including determining whether every pair of planar graphs on n vertices can be simultaneously embedded (with no bends). Closing the gap between the upper and lower bounds of the cardinality of a universal point-set for planar graphs with no bends allowed also remains open. When k bends per edge are permitted, universal point-sets of smaller asymptotic cardinality may be determined for $k = 1, 2$.

Acknowledgements

References

[1] M. Kurowski, A 1.235 lower bound on the number of points needed to draw all n-vertex planar graphs, Inf. Process. Lett. 92 (2) (2004) 95–98.
[2] M. Chrobak, H. Karloff, A lower bound on the size of universal sets for planar graphs, SIGACT News 20 (4) (1989) 83–86.
[3] H. de Fraysseix, J. Pach, R. Pollack, How to draw a planar graph on a grid, Combinatorica 10 (1990) 41–51.
[4] W. Schnyder, Embedding planar graphs on the grid, in: Proc. 1st ACM–SIAM Sympos. Discrete Algorithms (SODA'90), 1990, pp. 138–148.
[5] P. Gritzmann, B. Mohar, J. Pach, R. Pollack, Embedding a planar triangulation with vertices at specified points, Amer. Math. Monthly 98 (2) (1991) 165–166.
[6] M. Kaufmann, R. Wiese, Embedding vertices at points: Few bends suffice for planar graphs, Journal of Graph Algorithms and Applications 6 (1) (2002) 115–129.
[7] H. Everett, S. Lazard, G. Liotta, S. Wismath, Universal sets of n points for one-bend drawings of planar graphs with n vertices, Discrete and Computational Geometry 43 (2) (2010) 272–288, http://hal.inria.fr/inria-00431769/en.
[8] E. Di Giacomo, W. Didimo, G. Liotta, S.K. Wismath, Curve-constrained drawings of planar graphs, Computational Geometry 30 (2005) 1–23.
[9] P. Bose, On embedding an outer-planar graph on a point set, Computational Geometry: Theory and Applications 23 (2002) 303–312.
[10] G. Di Battista, P. Eades, R. Tamassia, I.G. Tollis, Graph Drawing, Prentice Hall, NJ, 1999.
[11] J. Valdes, R.E. Tarjan, E. Lawler, The recognition of series-parallel digraphs, SIAM J. Comput. 11 (2) (1982) 298–313.
[12] G. Di Battista, G. Liotta, F. Vargiu, Spirality and optimal orthogonal drawings, SIAM J. Comput. 27 (6) (1998) 1764–1811.
[13] P. Braß, E. Cenek, C.A. Duncan, A. Efrat, C. Erten, D. Ismailescu, S.G. Kobourov, A. Lubiw, J.S.B. Mitchell, On simultaneous planar graph embeddings, Comput. Geom. 36 (2) (2007) 117–130.